Colonocyte keratins are up-regulated in hypoxia and affects the nuclear translocation of HIF-1a

Aruna Ghimire

Master's thesis

Åbo Akademi University
Biomedical Imaging
21.03.2019

Master's in Biomedical Imaging
Microscopy

Credits: 45 ECTS

Supervisors:
1: Diana Toivola (Assoc. Prof)
2: Iris Lähdeniemi (PhD)
3: Terhi Helenius (PhD)

Examiners:
1:
2:

ÅBO AKADEMI UNIVERSITY

Department of Biosciences

Faculty of Science and Engineering

ARUNA GHIMIRE: Colonocyte keratins are up-regulated in hypoxia and affects the nuclear translocation of HIF-1a

Master's thesis, 65 pp., 1 Appendix

Microscopic Imaging

March 2019

The cytoskeleton is divided into three types: microtubules, microfilaments and intermediate filaments (IFs). IFs are further divided into six different types. The first two types of IFs are type I and type II keratins. Keratins provide mechanical and non-mechanical strength to epithelial cells and they also protect cells from various types of stress. Both type I keratins (K18, K19 and K20) and type II keratins (K7 and K8) are present in colon. Keratins such as K7 and K20 are up-regulated under intestinal stress. During hypoxia (inadequate supply of oxygen (O_2) to the cells), colonic epithelium expresses a transcriptional factor, hypoxia inducible factor-1 alpha (HIF-1a). Hypoxia inducible factor-2a (HIF-2a) is also a transcriptional factor expressed in colon and has a regenerative function. The hypothesis of this study was that the cells react to hypoxia by up-regulation of keratins, similar to stress. It was also hypothesized that keratins modulate hypoxia signaling pathway in colon. To understand how keratins and the hypoxia signaling pathway are regulated, protein analysis, immunofluorescent staining, confocal imaging and image analysis were performed. This study found that HIF-1a and HIF-2a are down-regulated in absence of K8 in basal colon of mice. In addition, K19 and K20 are up-regulated in hypoxic condition in mouse colon and colon cancer cells. Moreover, *in vitro* hypoxia study of the CRISPR/Cas9 Caco-2 cell showed up-regulation of HIF-1a more in $K8^{-/-}$ cells compared to $K8^{+/+}$ cells. Similarly, HIF-1a translocate to nucleus more in $K8^{-/-}$ compared to $K8^{+/+}$ cells. In conclusion, keratins are up-regulated in hypoxia and keratins regulate HIF signaling pathway.

KEYWORDS: Keratins, hypoxia, normoxia, HIFs, microscopy, nuclear translocation

Abbreviations

AGT	alkylguanine-DNA-alkyltransferase
BC	benzylcytosine
BCA	bichronic acid
BG	benzylguanine
BMI	body mass index
BMP	bone morphogenetic protein
BSA	bovine serum albumin
Caco-2	caucasian colon adenocarcinoma
CD	Crohn's disease
Cl-	chloride ion
CO_2	carbondioxide gas
$CoCl_2$	cobalt chloride
CRC	colorectal cancer
CRISPR	clustered regularly-interspaced short palindromic repeats
Cu^+	cupper ions
dH_2O	distilled water
DMEM	Dulbecco's modified eagle medium
DMOG	dimethyloxaloylglycine
DMSO	dimethylsulfoxide
DRA	down-regulated in adenoma
EBS	epidermolysis bullosa

ECL	electrochemiluminiscence
EDTA	ethylenediaminetetraacetate
EPO	erythropoitien
ER	endoplasmic reticulum
HFD	high fat diet
HIF-1a	hypoxia inducible factor-1alpha
HIF-2a	hypoxia inducible factor-2alpha
HOX	hypoxia
i.p	intra peritoneal
IBD	inflammatory bowel disease
IF	intermediate filament
K	keratin (similarly, K8 stands for keratin 8)
LCSM	laser scanning confocal microscope
MUC-2	mucin-2
N_2	nitrogen gas
Na+	sodium ion
NDS	normal donkey serum
NF	neurofilament
NGS	normal goat serum
NOX	normoxia
NP-40	nonylphenoxypolyethoxylethanol-40
O_2	oxygen gas

OCT	optimum cutting temperatre
PBS	phosphate buffer saline
PFA	paraformaldehyde
PHD	prolyl hydroxylases
PTM	post-translational modifications
PVDF	polyvinylidene difluoride
RT	room temperature
SDS-PAGE	sodium dodecyl sulphate polyacrylamide gel electrophoresis
SEK	simple epithelial keratin
TA	transient amplifying
UC	ulcerative colitis
VEGF	vascular endothelial growth factor
VHL	Von Hippel Lindue

Contents

1. Review of the literature

1.1 The colon

The colon is a part of the digestive system and it is about 1.5 m long in humans (Rao and Wang, 2010). The colon is situated in between caecum and rectum. The human colon is divided into four parts: ascending colon, transverse colon, descending colon and sigmoid colon (Bhimji and Gossman, 2017). In mice, the colon is divided into two parts: proximal colon (towards small intestine) and distal colon (towards rectum) (Asghar et al., 2015). The major function of the colon is to absorb water and electrolytes after the digestion of the food in the small intestine (Motte et al., 2003; Steegenga et al., 2012). The colon also plays an important role as a barrier between the immune system and the gut microbiota (Garrett et al., 2010).

The colon harbours a dense amount of commensal bacteria that live in the intestinal tract in symbiosis with the host. The intestinal tract benefits from the microbiota in digestion of food materials in exchange with some of the food nutrients digested with the help of the microbiota (Johansson et al., 2011). The mechanisms in the symbiosis are not clearly understood. However, a low supply of oxygen in the lumen of the colon is commutable for the bacterial community (Byndloss and Bäumler, 2018). A low supply of oxygen in the colon epithelium also limits the function of microbiota. Dysbiosis, an imbalance in the symbiosis, may lead to non-communicable diseases in the human, such as inflammatory bowel disease (IBD), which are characterized by variations in the microbial composition (Byndloss and Bäumler, 2018). The bacterial communities in the colon are diverse among their species. One individual might have different bacterial species in their colon than another individual (Johansson et al., 2011).

1.1.1 Tissue layers and cells in colon

Similar to the other part of the intestinal tract, the colon wall consists of four layers of tissue: the mucosa is the innermost layer (consists of epithelium, lamina propria and muscularis mucosa), the sub-mucosa, the muscularis propria and the serosa (outermost layer). The mucosa layers in the colon are thicker compared to the small intestine. The cells in mucosa and sub-mucosa layers produce proteins such as mucin and glycoproteins. These proteins protect the colon against microbial invasion inside the tissue layers of the colon (Okumura

and Takeda, 2017). The muscularis propria consists of myentic plexus (mesh of neural fibre and ganglionic cluster). It is peristaltic in function, pushing down the food material in the gut lumen (Rao and Wang, 2010). Each layer is connected with one another by connective tissue throughout the intestinal tract (Rao and Wang, 2010).

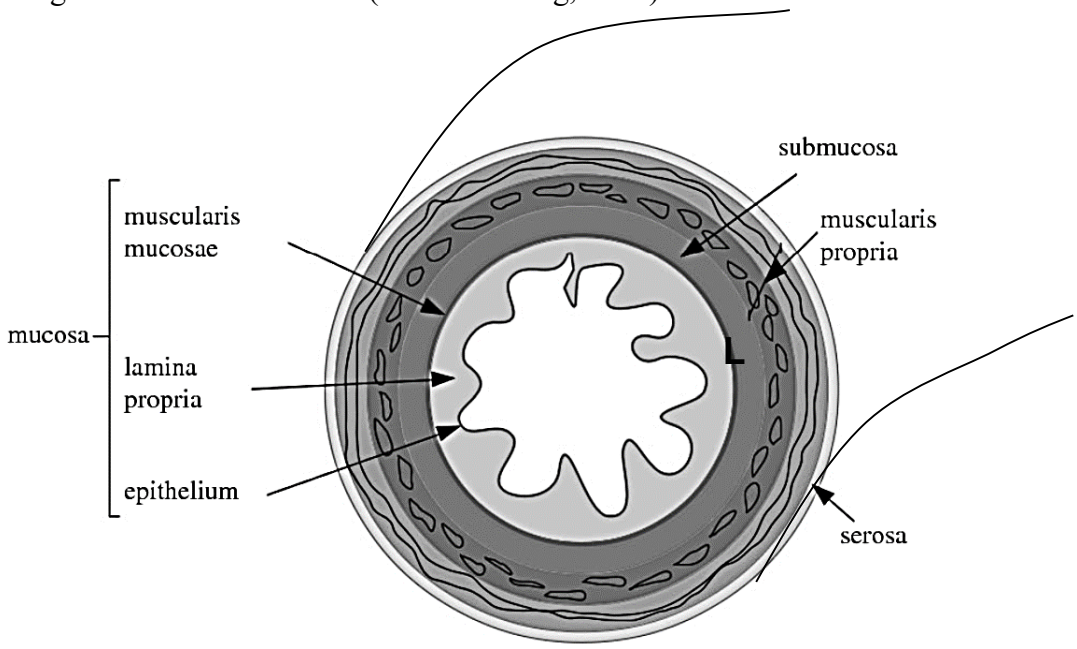

Figure 1. The organization of tissue layers in the colon. The outer tissue layer of the colon is lined with the serosa. Beneath the serosa lies the muscle layer, which is continuous with the sub mucosa. The muscularis propria is present underneath the sub mucosa which is continuous with innermost layer, the epithelium, lining the colon lumen (L). Picture modified from Balbi and Ciarletta, 2013.

The colonic epithelium consists of stem cells which are reconstructive or regenerative in function. The stem cells divide to produce transit amplify (TA) cells which further divide and differentiate to other colonic epithelial cells: absorptive enterocytes, mucus producing goblet cells, paneth cells (mainly located in small intestine) and epithelium M-cells (Garrett et al., 2010; Wells et al., 2011). The differentiation and proliferation of the colon epithelium are maintained by different signaling pathways such as Wnt, bone morphogenetic protein (BMP), Notch, Eph/ephrin, Hippo and Hedgehog signaling pathway (Meran et al., 2017). All epithelial cells are mainly digestive and absorptive in function. They also protect colon against microbes invasion (Garrett et al., 2010; Wells et al., 2011). Unlike the small intestine, the colon epithelium lacks villi, which provide higher surface area for absorption. Instead, the colon epithelium has folded crypts. The colon has a large number of goblet cells and have a thicker mucus layer which plays an important role as a barrier against the microbes. The

goblet cells produce and polymerize gel-forming mucin-2 (MUC2), which is one of the major proteins that prevent the invasion of the microbiota (Johansson et al., 2011).

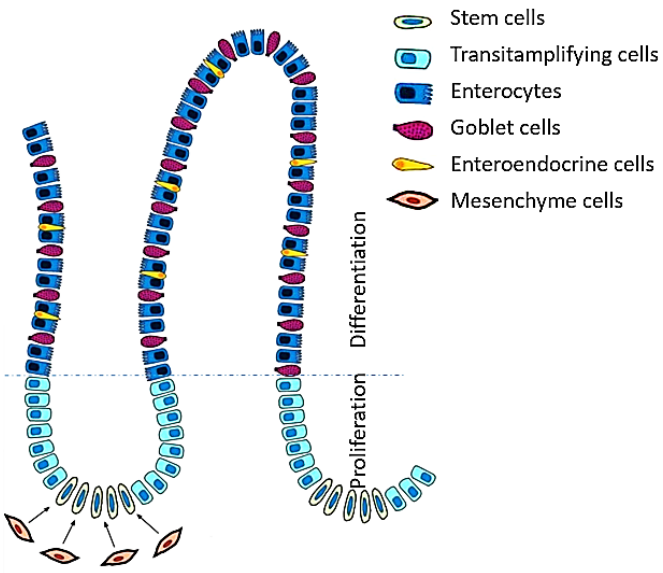

Figure 2. Different types of cells in colon epithelium. The colon epithelium consists of stem cells, which further produce transit amplifying cells. The transit amplifying cells differentiate into goblet cells, enterocytes, mesenchyme cells and enteroendocrine cells. Picture modified from Di Franco et al., 2011.

1.1.2 Diseases in colon

Colorectal cancer (CRC) is the third most common type of cancer causing death in men and second most common in women in the world (Rossi et al., 2018). It is one of the major diseases of colon along with inflammatory bowel disease (IBD) (Motte et al., 2003; Wu et al., 2017). CRC arises from the intestinal epithelium and is associated with genetic and epigenetic transformations leading to cancer due to change in signalling cascade such as hedgehog and Wnt signalling pathway (Planutis et al., 2014; Wu et al., 2017).

The most common forms of IBDs are Crohn's disease (CD) and ulcerative colitis (UC). Both CD and UC can be caused by genetic factors, environmental factors or mucosal dysfunction. They are also induced by the change in species diversity of the microbiota of the intestinal tract (de Mattos et al., 2015). CD and UC are distinguished on the basis of the site of the occurrence of inflammation. CD can occur towards the end of the small intestine and the proximal colon, while UC occurs in the distal end of the colon (Narula and Fedorak, 2008). Although the exact physiology of IBD is not fully understood, oral medication, drug targeted

therapies, anti-TNF therapies, anti-integrin therapies and surgical procedures are available to treat the disease. The influence of the treatment may depend on the genotype and immunity or response to drug, of the patient (Regueiro et al., 2016).

1.2 Cytoskeleton

The cytoskeleton is a network of filamentous structures present in the cell. In eukaryotes, the cytoskeleton consists of three main types of structures: microtubules, microfilaments and intermediate filaments (IFs) (Alberts et al., 2007).

Microtubules are composed of a protein called tubulin. Tubulin monomers (a-tubulin and b-tubulin) bind to each other and form a polypeptide chain (Alberts et al., 2007). Microtubules are important protein structures for cellular mechanisms such as, cell division and intracellular transportation (Alberts et al., 2007; Li et al., 2015). They are also involved in maintaining the structure and function of the endoplasmic reticulum (ER) (Smyth et al., 2007).

Microfilaments are composed of the protein called actin. Actin filaments are found dispersed throughout the cells but are highly concentrated under the plasma membrane of animal cells. They provide strength and shape to the lipid bilayer in the plasma membrane. They are important in regulating cell movement and cell division. They are also associated with myosin, in their contractile function of the cell (Alberts et al., 2007). Actin binds to proteins such as β-spectrin and α-actinin (Norwood et al., 2000) to form a filamentous structure.

Microtubules and microfilaments consist of mainly one type of proteins each, while IFs consist of many different proteins. Over 70 different IF genes have been found in total and all IFs are classified into six different types. The classification of IFs is based on their location in the cell (Omary, 2009). The first two types of IFs are type I and type II keratins. The third type of IFs includes proteins such as vimentin, desmin, glial fibrillary acidic protein and periferin. The fourth types of IFs are neurofilament proteins (NF) such as low NF (NF-L), medium NF (NF-M), high NF (NF-H), nestin and α-internexin. The nuclear lamins are the fifth type of IF proteins whereas filensin and phakinin are the sixth types of IFs, found more specifically in the eye lens (Cooper, 2000; Oshima, 2007). The overall classification table of IF proteins along with their primary cell and tissue expression is listed in table 1. In this thesis

project the first two types of Ifs, type I and type II keratins, are studied and they are further described in section 1.3.

Table 1: IFs are present in different cells and tissues which are classified into six different types. Table modified from Omary, 2009.

Type of IF protein	Proteins	Primary cell/tissue
I (including hair keratins)	K9-K28, K31-K40	Epithelial and epidermal appendages
II (including hair keratins)	K1-K8, K71-K86	Epithelial and epidermal appendages
III	Vimentin GFAP Desmin Syncoilin Peripherin	Mesenchymal cells and lens Astrocytes Muscle Muscle (mainly skeletal/cardiac) Peripheral nervous system
IV	Neurofilaments (L, M, H) Internexin Nestin Synemin	Central nervous system Central nervous system Neuroepithelial cells Muscle
Nuclear V	Lamins	Nuclear lamina
Lens VI	Bfsp1 and Bfsp2	Fiber cells

1.3 Structure and function of keratins

Keratins are the largest type of IF proteins and they are the most abundant and diverse type of IFs. There are 54 different keratin genes in human cells (Toivola et al., 2015). All keratin filaments are categorized into type I (acidic) and type II (basic to neutral) keratins. Examples of type I keratins are K9, K10, K12, K13, K14, K15, K16, K17, K18, K19 and K20 and type II keratins are K1, K2, K3, K4, K5, K6, K7 and K8. Type I keratins copolymerize with type II keratins to form an obligate heteropolymer (Karantza, 2011).

Analysis of the keratin sequence revealed that it consists of three parts: the head, the tail and the central/rod domain. The N-terminal head domain and C-terminal tail domain are non-helical. The central rod domain is α- helical coil, which is further divided into four subdomains 1A, 1B, 2A and 2B. Linkers L1, L12 and L2 connect the subdomains of the rod

to each other. The non-helical domains form globular structure to interact with other proteins or molecules in the cytoskeleton (Bragulla and Homberger, 2009).

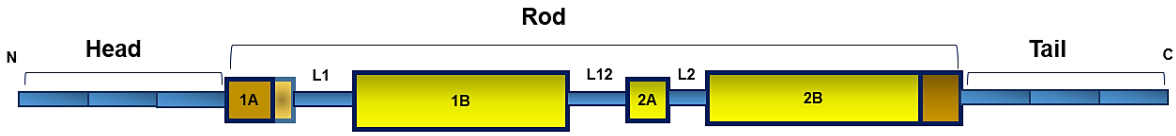

Figure 3. The structure of keratin has three domains: head, rod and tail. The head is N terminal and tail is C terminal. Both head and tail domain are non-helical. The α-helical rod domain is further divided into sub domains. In the figure, 1A, 1B, 2A and 2B are four α-helical sub-domains connected by linker domains (L1, L12 and L2) of the rod. Figure modified from Bragulla and Homberger, 2009.

Keratins are present throughout the cytoplasm and provide mechanical support to the cells. They are very dynamic and undergo filament modification due to stress (Kellner and Coulombe, 2009; Toivola et al., 2015). Keratins protect cells against stress and play roles in cell proliferation, growth, apoptosis and transport of cellular component (Kellner and Coulombe, 2009; Toivola et al., 2000). Keratins also regulate cell growth and protein synthesis (Kellner and Coulombe, 2009). Keratins are up-regulated and protect cells against stress in colon (Helenius et al., 2016).

1.3.1 Simple epithelium keratins in cells and tissues

Simple epithelial keratins (SEKs) are mostly found in the single cell epithelial lining of organs, such as colon, intestine, liver and pancreas, which have functions in secretion and absorption of enzymes and nutrients (Ku and Omary, 2006). SEKs that are found in simple epithelial cells are K7, K8, K18, K19, K20 and K23 (Figure 4). SEKs are expressed throughout the colon crypt. The major type of keratins present in the colon are K8, K18 and K19 which are present in both top (epithelial surface) and bottom of the crypt (crypt base) (Toivola et al., 2015; Zhou et al., 2003). In minority, K7 and K20 are also present in the colon, where K7 is mostly present towards the crypt base and K20 in the top part of the crypt. K7 and K20 are up-regulated when subjected to stress in the mice colon (Helenius et al., 2016).

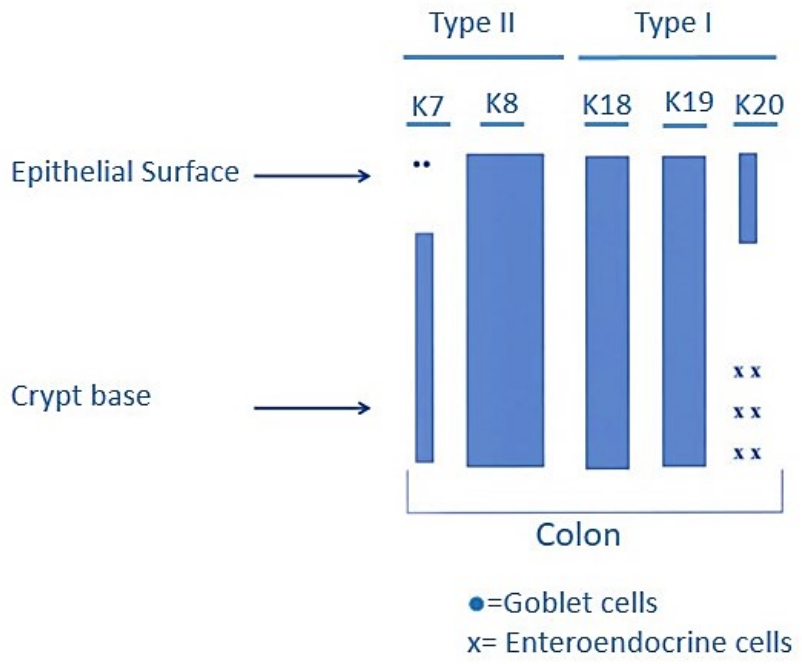

Figure 4. Type I and type II keratins are expressed in the colon epithelium. K8 is the major type II keratin expressed throughout the colon epithelium. K7 is also a type II keratin expressed in the colon, towards the crypt base. Type I keratins, K18and K19 are present throughout the colon crypt whereas K20 is expressed in top of the colon crypts. Picture modified from Zhou et al., 2003.

In addition to colon, SEKs are expressed in other organs and stratified/pseudo-stratified epithelia (for example respiratory and glandular epithelia) (Karantza, 2011). SEKs such as K7 and K19 are generally found in gastrointestinal epithelium. K20 is primarily found in gastric, urothelial and in Merkel cells (Omary et al., 2009). K23 is found in the cytoskeleton of the pancreatic cells (Bragulla and Homberger, 2009), liver and colon (Guldiken et al., 2016). Unlike the colon, K8 and K18 are the only type of SEKs in the human hepatocytes (Omary et al., 2009).

The importance of SEKs is described by the K8 null ($K8^{-/-}$) mouse model, which has a clear phenotype as it possess different diseases such as colitis, diarrhea and colonic hyper proliferation (Asghar et al., 2015; Baribault et al., 1994; Toivola et al., 2015). $K8^{-/-}$ mice have defects in their sodium (Na^{+}) and chloride (Cl^{-}) ion absorption and their transport in the colon (Asghar et al., 2015; Toivola et al., 2004). Down-regulated in adenoma (DRA), which is an essential anion exchanger in the intestine, is absent in $K8^{-/-}$ mice. The DRA molecules is also down-regulated in diseases, such as IBDs and colitis, which explains the protective role of keratins against such diseases (Asghar et al., 2016). In addition, K8 null-heterozygote mice

($K8^{+/-}$), which have 50% less keratin compared to $K8^{+/+}$ mice, do not have colon inflammation but they are more susceptible to the colitis under experimental conditions compared to $K8^{+/+}$ mice. Similarly, $K8^{+/-}$ mice have in-between level of Na^+ and Cl^- ion transportation in their colon compared to that of $K8^{+/+}$ and $K8^{-/-}$ mice, which illustrates the importance of keratin levels in protecting the colon epithelium (Asghar et al., 2015).

$K8^{-/-}$ mice also show altered regulation of the blood glucose level by reduced production of insulin in β-cells of the pancreas. The loss of keratins in the pancreas is also associated with irregular insulin vesicles and dysfunctional mitochondrial function due to decrease in mitochondrial surface proteins (Alam et al., 2013; Silvander et al., 2017). In addition, loss of keratin also alters the mitochondrial properties (such as protein profile, morphology and function) in liver (Tao et al., 2009). The liver of $K8^{-/-}$ mice is also more susceptible to FAS-mediated injury and apoptosis (Lee et al., 2013).

1.3.2 Post Translational modification of keratins

Keratins undergo different post translational modifications (PTMs) such as phosphorylation, glycosylation, acetylation, proteolysis and transglutamination (Snider and Omary, 2014). PTMs of keratins are associated with keratin organization, solubility and integrity. PTMs, such as phosphorylation occur within tail or head domain of keratins and it is the most studied modification of keratins (Snider and Omary, 2014). Keratins, such as K8 and K18, are mostly phosphorylated at serine residue and tyrosine/threonine residue (Toivola et al., 2002). Phosphorylated keratins are highly soluble and undergo structural reorganization. Keratin phosphorylation also promotes binding of the keratins to other proteins and apoptosis (Snider and Omary, 2014).

Keratin glycosylation has been identified in the head domain of K8, K18 and K13 (Herrmann and Harris, 1998). Keratin glycosylation protects epithelial cells against stress and injury by activating cell survival kinases and promote keratin phosphorylation. Similarly, acetylation of keratins, such as K8, occurs in the N-terminal and promotes keratin filament organization and modulation (Snider and Omary, 2014).

Proteolysis modification of keratin, such K18 and K19, is known to be associated with apoptosis (Ku et al., 1997; Omary et al., 1998; Snider and Omary, 2014). Keratin

transglutamination is known to have a protective role in physiological and pathological conditions (Herrmann and Harris, 1998).

1.4 Hypoxia and hypoxia inducible factors

Cells maintain their oxygen (O_2) level in order to regulate the cellular activities, such as cell growth, metabolism and regeneration. When the O_2 level is altered and becomes insufficient, cells undergo a hypoxic condition. Hypoxia in tissue is a condition of inadequate supply of O_2 by the circulatory system (Höckel and Vaupel, 2001). The atmospheric O_2 concentration (21%) is called normoxia. However a low amount of O_2 supplied to tissues during physiological conditions is called physioxia or tissue normoxia, such as 8% in the intestinal wall or 2% in the intestinal lumen (Zeitouni et al., 2016; Zheng et al., 2015). The O_2 concentration in the intestinal tissues is very fluctuating, depending on food intake and blood flow (Zeitouni et al., 2016). The O_2 level in the mice colon is extremely low, less than 2% (Albenberg et al., 2014). The receptors, such as carotid bodies (Prabhakar and Semenza, 2015), in the eukaryotic cells, sense high or low amount of O_2 and the response can be both acute and chronic (Michiels, 2004). When hypoxia is sensed, the mechanism to restore normoxia is activated. The mechanism to restore O_2 levels relies on transcription factors such as hypoxia inducible factor-1 alpha (HIF-1a), hypoxia inducible factor-2alpha (HIF-2a) or by prolyl hydroxylases (PHDs) (Eltzschig and Carmeliet, 2011), which hydroxylate HIFs (Chan and Vanhoutte, 2013).

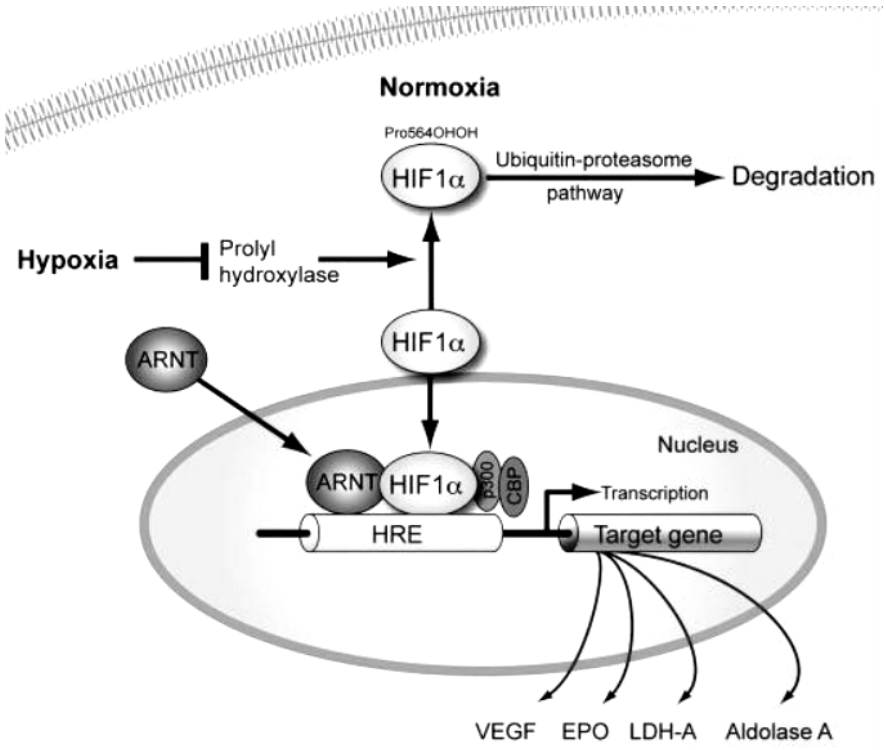

Figure 5. HIF-1a signaling pathway during normoxia and hypoxia. In normoxia, HIF-1a undergoes degradation via hydroxylation by PHDs and undergoes further degradation by the ubiquitin-proteosomal pathway, which is mediated by VHL. In hypoxia, HIF-1a is more stable and localizes to the nucleus, binds to its heterodimer HIF-1b and activates the target genes such as VEGF, EPO and others. Picture modified from Xia et al., 2009.

Oxygen dependent molecules, such as PHDs and factor inhibiting HIF-1a (FIH-1), regulate the degradation of HIF-1a in normoxic conditions. PHDs are activated in normoxia and hydroxylate (addition of hydroxyl (OH) group) HIF-1a. Hydroxylated HIF-1a undergoes ubiquitination which is mediated by Von Hippel Lindue (VHL) (Dengler et al., 2014; Eales et al., 2016). When oxygen level falls very low, PHDs are inactivated and then HIF-1a stabilizes and translocate to the nucleus. The non-hydroxylated HIF-1a, in the nucleus, pairs with the β-subunit (HIF-1b) and initiates the gene transcription (Muz et al., 2015). HIF-1a and HIF-2a have different target genes as their phenotypes for deficiency of each transcriptional factors differ from each other (Eltzschig and Carmeliet, 2011). Both HIF-1a and HIF-2a induce target genes, such as erythropoietin (EPO) and vascular endothelial growth factor (VEGF), transcription under hypoxia and mediate cell migration, survival, differentiation, metabolism and apoptosis. Both HIFs can show similar cellular response to the hypoxia or can be selective with their target gene activity and exhibit cell type specific

regulation (Dengler et al., 2014; Zhu et al., 2016). During hypoxia, HIF-1a is mostly associated with angiogenesis while HIF-2a is associated with erythropoietin production for the vascular supply (Chan and Vanhoutte, 2013; Eltzschig and Carmeliet, 2011).

Both HIFs are stabilized in IBD and CRC (Chan and Vanhoutte, 2013; Eltzschig and Carmeliet, 2011). In CRC, HIF-1a modulates firmness and malignancy of the cancer (Santoyo-Ramos et al., 2014) and HIF-2a regulates growth and progression of the cancer (Ma et al., 2017).

HIF-3a in cancer biology is not studied very much but it is known to be down-regulated in renal cancer and has a different role than HIF-1a and HIF-2a in general (Majmundar et al., 2010). Most likely, HIF-3a is more correlated to obesity and expression in adipose tissue. The higher the expression of HIF-3a in adipose tissue, higher is the body mass index (BMI) and obesity related traits (Pfeiffer et al., 2016).

1.4.1 HIFs induction with chemical treatment

Cobalt chloride ($CoCl_2$) is a chemical compound that exhibits the property of mimicking hypoxia by stabilizing HIF-1a. It is not completely known how the compound interacts biologically but the cobalt in $CoCl_2$, binds to the iron-binding site of PHDs and inactivates them. Inactivated PHDs cannot hydroxylase HIF-1a and HIF-1a becomes more stable in the cells (Yuan et al., 2003). Cobalt also inhibits pVHL mediated degradation of HIF-2a by binding to the VHL-binding domain of HIF-2a (Yuan et al., 2003). Dimethyloxalyglycine (DMOG) is also a hypoxia mimetic and is a direct inhibitor of mitochondrial function and cellular respiration. Similar to the $CoCl_2$, DMOG inhibits the function of PHD and therefore stabilizes HIF-1a in the cells (Zhdanov et al., 2015).

1.5 Techniques of labeling: SNAP and CLIP fluorescent tags

Genetically encoded fluorescent fusion tags are used for imaging of the cells to understand the function and regulation of biological molecules that are present inside the cells. The fluorescent tags or the probe are being developed along with the development of imaging technologies and they are already in use to label proteins for cellular imaging of the live cells (Crivat and Taraska, 2012).

SNAP tag is a self-labeling protein tag, which binds to the corresponding labeling substrate via covalent bonding. It is a modified form of DNA repair enzyme of human O^6-alkylguanine-DNA-alkyltransferase (AGT) and it can form a stable bond with synthetic O^6-benzylguanine (BG) derivatives. SNAP tag can be attached to a protein of interest at gene level (SNAP tag fusion), without modifying the property of the specific protein (Cole, 2013). SNAP tag fusion can be labeled at the cell surface or can be transfected into the cells and labeled with cell permeable substrate to track the protein (Cole, 2013). During the substrate reaction, the SNAP fusion protein tag binds with its consecutive substrate leaving guanine in the cytoplasm (Gautier et al., 2008). SNAP tag provides high sensitivity and specificity for labeling of the protein with less background (Gautier et al., 2008).

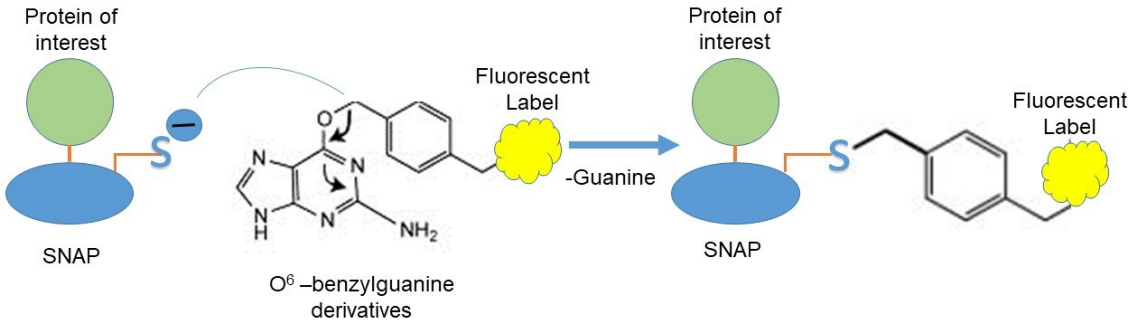

Figure 6. A protein of interest is fused with SNAP tag. The SNAP tag binds with label by covalent bonding with the O^6 –benzylguanine derivative, leaving out the guanine during the reaction. Picture modified from Cole, 2013.

Similar to the SNAP tag, a CLIP tag is a modified form of DNA repair enzyme of human O^2-alkylcytocine-DNA alkyltransferase, which can covalently bind to O^2-benzylcytosine (BC) substrate. It can also bind to protein of interest and it can be labeled with other fluorescent molecules (Liss et al., 2015). SNAP tag can be labeled along with CLIP tag and can simultaneously bind to different substrates, and can access tracking of different proteins in single experiment (Cole, 2013). Labeling of proteins with such synthetic probes is being a powerful tool of molecular biology (Gautier et al., 2008).

2. Aims and hypothesis

The purpose of this thesis project is to understand the role of colonocyte keratins under hypoxic condition and their influence on the HIFs signaling pathways. The major three aims of this project are as follows:

1. To determine the effects of hypoxia on colonocyte keratins.
2. To determine if keratins regulate the HIF signaling pathways in the colon.
3. To determine the dynamic localization of HIF proteins under hypoxia in the absence of K8 using SNAP/CLIP fluorescent tags.

In addition to above three major aims, two sub aims were generated during experimental analysis and were studied briefly in this thesis. The sub aims are as follows:

1. To determine if the level of keratins change with increasing passage in CRISPR/Cas9 Caco-2 $K8^{+/+}$ and $K8^{-/-}$ cells.
2. To determine the effect of culture medium on HIF-1a regulation when incubated for different time period in CRISPR/Cas9 Caco-2 $K8^{+/+}$ and $K8^{-/-}$ cells.

The hypothesis of this project is that keratins modulate the hypoxia signaling pathway and hypoxic stress alters the keratin levels in the colonic epithelium.

3. Materials and Methods

3.1 Animals

The mice used for the thesis project were wild type ($K8^{+/+}$) and $K8^{-/-}$ mice of FVB/n background. All mice that were experimented with hypoxia treatment were kept in animal care facility in Chicago, USA, and handled under the animal experiment license of Karen's Ridge laboratory. Mice experimented to study HIFs levels were kept in animal facility of the University of Turku and experimented under license ID ESAVI/4199/04.10.07/2014 provided by the National Animal Ethics Committee in Finland. The genotypes of the mice were confirmed by the polymerase chain reaction (PCR) method (Baribault et al., 1994) and western blot analysis.

3.2 CRISPR/Cas9 CaCo-2 cell line and culture

Colorectal adenocarcinoma cell (Caco-2) lines are the cells obtained from human colon adenocarcinoma. These cell lines form a monolayer of cells when cultured in a culture dish and exhibit morphological and functional properties of enterocyte (Sambuy et al., 2005). Clustered regularly-interspaced short palindromic repeats/Cas9 (CRISPR/Cas9) Caco-2 cells are modified colorectal adenocarcinoma cell. The *KRT8* gene, which produces K8 protein in the cells, was removed by the CRIPSR/Cas9 method to produce $K8^{-/-}$ cells (Misiorek et al., 2016). For the *in vitro* experiment, the CRISPR/Cas9 Caco-2 $K8^{+/+}$ and CRISPR/Cas9 $K8^{-/-}$ cell lines were used. The cells were cultured in a normal incubator at 37 ºC, supplied with 5% CO_2 and humidification (normoxia or NOX). The culture medium was prepared using 500 ml of Dulbecco's modified eagle medium (DMEM) (Biowest, France) with 20% fetal bovine serums (FBS), 2 mM L-glutamine and 100 µM penicillin and streptomycin. The cultures were splitted when the confluency of the cells was around 70% to 80%. During each split, the cells were first washed twice with 1X PBS and were then treated with trypsin (Biowest, France) (containing 0.25% EDTA), to detach them from the culture plate. After 5 minutes of incubation with trypsin, fresh medium was added to the cells, which were sub-cultured in a new cell plate (which formed a new passage each time). The ratio of split for the $K8^{+/+}$ was 1:4, while $K8^{-/-}$ was 1:3 on each passaging due to the variance in the growth rate between $K8^{+/+}$ and $K8^{-/-}$ cells ($K8^{+/+}$ cells divide faster than $K8^{-/-}$).

3.3 Hypoxia induction

Hypoxia was induced within a hypoxia chamber Invivo2 Hypoxia Workstation (Baker Ruskinn, UK). The chamber itself needed preparation time for the hypoxic condition and was turned on for an hour (h) prior to the experiment. The O_2 percentage was set to 8% for *in vivo* and 1% for *in vitro* experiment to induce hypoxia (HOX). For the *in vivo* experiment, the mice were placed in the hypoxia chamber and the O_2 percentage was gradually decreased from 21% to 8% O_2 (with 99.5% pure N_2) and hypoxia was generated. The mice were kept in the hypoxia chamber for 4 hours and 24 hours, after the oxygen concentration was set to 8%. Mice were also kept in normoxic condition with 21% O_2 (NOX or control) for comparative study. After 24 hours, the mice were sacrificed by intraperitoneal (i.p) injection of euthasol. Distal and proximal ends of the colon were collected in OCT and middle of the colon was lysed in homogenization buffer.

Similarly for *in vitro* experiments, both CRISPR/Cas9 Caco-2 $K8^{+/+}$ and CRISPR/Cas9 Caco-2 $K8^{-/-}$ cells were treated for 4 hours inside the hypoxia chamber (supplied with 1% O_2, 5% CO_2 and the rest with 99.5% pure N_2). After hypoxia treatment, cells were washed twice with 1X phosphate buffered saline (PBS), lysed with 100 µl of homogenization buffer and collected into eppenderf tubes. The collected samples were boiled at 95 ºC for 5 minutes and stored in a -80 ºC freezer. Cells grown on coverslip were also incubated in the hypoxia chamber at the same time, washed twice with 1X PBS and fixed with 4% PFA for 20 minutes in room temperature (RT) and stored in +4 ºC in PBS. Both $K8^{+/+}$ and $K8^{-/-}$ cells were also incubated in normoxic conditions to perform a comparative study.

3.3.1 Chemical treatment to induce HIFs

For the *in vivo* experiment, DMOG treatment was used to chemically induce HIF-1a in $K8^{+/+}$ mice. The mice were treated with 8 mg of DMOG (dissolved in DMSO), by i.p injection, and colon samples were collected after 48 hours of the treatment. For comparative study, mice were also treated with 100 µl of DMSO (control) at the same time and samples were collected similarly to the hypoxia treatment experiment.

For *in vitro* study, 400 µM $CoCl_2$ was used to induce HIF-1a in the CRISPR/Cas9 Caco-2 cells. The $CoCl_2$ treatment was carried out when the cells had reached 80% confluency. The samples were collected similarly to the hypoxia treatment experiment after 4 hours of the

$CoCl_2$ treatment. For comparative study, cells were also treated with 34 µl of DNA/RNA free sterile water in 51 ml of medium as control. For live cell imaging, 100 µM $CoCl_2$ was used to observe nuclear translocation of HIF-1a.

3.4 Sample preparation

3.4.1 Tissue sample preparation

From the *in vivo* hypoxia experiment, parts of distal and proximal colon of the mice were collected in optimum cutting temperature (OCT) compound and frozen fresh for tissue section analysis. The middle part of the colon was lysed in homogenization buffer for further protein analysis. To the homogenization buffer, 1% protease inhibitor (P.I) cocktail and 2% phenylmethylsulfonyl fluoride (PMSF) were added in order to prevent protein degradation. All samples were grinded using Potter-Elvehjem tissue grinder by moving piston up and down for multiple times, until fine pieces, which were invisible to naked eye. Samples were then boiled at 95 ºC for 5 minutes and were stored at -80 ºC until further application such as protein assay.

3.4.2 Cell sample preparation

3.4.2.1 Protein assay

Protein assay was done using the bicinchoninic acid (BCA) assay method (Thermo Scientific, Waltham, MA, USA). It uses the formation of cupper ions (Cu^+) by using BCA in the protein solution, which forms a purple blue color under alkaline condition (Huang et al., 2010). The protein concentrations were then measured, using 562 nm absorption spectrum of a spectrophotometer (Wallac Victor^{2TM}, Perkin Elmer), based on the intensity of the color formed in each well.

For the measurement, first the samples were diluted 1:10 ratio in distilled water (dH_2O). A triplicate of each samples (25 µl each) were loaded to 96-well plate. A set of standards of bovine serum albumin (BSA), with known concentrations, was also loaded on the same well plate. Since the samples were all lysed in homogenization buffer, the buffer was diluted as samples and loaded in the plate as a blank. The BCA kit reagent (A and B) was diluted in the ratio B:A=1:50. 200 µl of the reagent mixture was added to all standards, samples and the blank. The microplate was then incubated at 37°C for 30 minutes and again for 10 minutes

at RT in dark. The final concentration of the samples were determined on the basis of the standard curve plotted on Microsoft Excel (Microsoft Corporation, USA), where absorbance is plotted against known protein concentrations of standards. The absorbance of the blank was subtracted from all standards and samples in order to avoid absorbance due to homogenization buffer. Samples were then diluted with 3X Laemmli sample buffer, containing SDS, which denatures the protein in the sample, so that the concentration of each sample was 5 µg/10µl of proteins, on the basis of the standard curve.

3.5 SDS-PAGE

Sodium dodecyl sulphate polyacrylamide gel electrophoresis (SDS-PAGE) is a method of gel electrophoresis, used for separating the proteins in a biological sample on the basis of their molecular weight (Nowakowski et al., 2014).

For SDS-PAGE, equal amounts of samples (10 µl /well) were loaded on a polyacrylamide gel for electrophoresis. Samples were loaded on 10% polyacrylamide gel for different keratin proteins, while for higher molecular weight protein, such as HIF-1a (120 kDa), 7% gels were used. The gel contains lower and upper gel. The upper gel contains low concentration of polyacrylamide, which is more porous than the lower gel. The upper gel allows the free movement of all proteins to reach the lower gel. The lower gel is dense and has higher pH compared to upper gel and proteins will start to migrate according to their molecular weight (Wilson and Walker, 2009). For this thesis project 7% and 10% lower gels were used with 4% stacking or upper gels (table 2).

Table 2. The exact contain of different percentage acrylamide gels used for this thesis project.

Acrylamide concentration	**10% Lower gel**		**7% Lower gel**		**4% Upper gel**	
1mm gels	2 gels (ml)	4 gels (ml)	2 gels (ml)	4 gels (ml)	2 gels (ml)	4 gels (ml)
Lower gel stock (pH 8.8)	2.250	4.500	2.250	4.500	-	-
Upper gel stock (pH 6.8)	-	-	-	-	1.250	2.250
20% SDS	0.045	0.090	0.045	0.090	0.025	0.050
Acrylamide stock	3.000	6.000	2.100	4.200	0.750	1.500
dtH2O	3.750	7.500	4.650	9.300	3.000	6.000
10% APS	0.060	0.120	0.060	0.120	0.020	0.040
TEMED	0.006	0.012	0.006	0.120	0.010	0.020

During gel electrophoresis, a voltage of 100 V was applied to the gel in a solution of running buffer. The running buffer contains SDS, a negatively charged detergent, which promotes denaturation of the protein's tertiary structure. SDS interacts with the hydrophobic tail of proteins, making them negatively charged and prevents tangling of the protein to make them run efficiently in the gel. The negatively charged linear proteins in the gel move towards the positive potential (the base of the gel). The protein molecules with lower molecular weight will migrate faster and lower in the gel than the proteins with higher molecular weight (Nowakowski et al., 2014). A protein marker with known band sizes was used to identify the protein of interest. The electrophoresis of the gel was continued until the marker reached the bottom of the gel.

3.5.1 Transfer and western blot

The proteins on the gel were then transferred to a methanol-activated polyvinylidenedifluoride (PVDF) membrane by the wet transfer method, where the membrane was placed towards the positive terminal of the supplied voltage and the gel towards the negative terminal. The transfer was carried out at +4°C temperature for 1 hour, at 100 V in a transfer buffer.

After the transfer, the PVDF membrane (with proteins on it) was washed once with 5 ml of 0.2% PBS-Tween for 1 minute, to remove excess methanol. The membrane was then blocked with 5% fat-free milk in 0.2% PBS-Tween for 1 hour in RT, to prevent unspecific binding of the antibodies.

After blocking with milk, the membrane was washed three times within 15 minutes with 0.2% PBS-Tween, to remove excess milk from the membrane. The membrane was then incubated with a specific primary antibody for 1 hour at RT, washed three times (5 minutes each) with 0.2% PBS-Tween and incubated with a secondary antibody conjugated to horse radish peroxidase (HRP) from a corresponding host for 1 hour in RT. The primary and secondary antibodies used for different proteins are listed in table 3 and table 4.

Table 3. **The list of primary antibodies used for immunoblotting in this thesis project**.

Antibody	Host	Concentration	Manufacturer	Product number	Molecular weight (kDa)
K7 (RCK-105)	Mouse	1:500	Abcam	ab9021	50.6
K8 (Troma I)	Rat	1:10000	Developmental studies Hybridoma Bank	-	54.1
K18 (275, J. Eriksson)	Rabbit	1:10000	John Erikson Laboratory	-	47.4
K19	Mouse	1:1000	Sigma	C7159	40
K20 (IT-Ks20.8)	Mouse	1:1000	Progen	AB_531826	48.9
HIF-1a	Mouse	1:500	NovusBiologica	NB 100-105	116
HIF-1a	Rabbit	1:1000	Novus Biologica	NB 100-134	120
HIF-2a	Rabbit	1:1000	NovusBiologica	NB 100-122	110
B-actin	Rabbit	1:1000	Cell Signalling	-	42
Hsc70 (IB5)	Rat	1:5000	Stressgen	61054	73

Table 4. **The list of secondary antibody used for immunoblotting in this thesis project.**

Antibody	Host	Concentration	Manufacturer	Product number
Anti-mouse HRP	Sheep	1:10000	GE healthcare	NA931
Anti-rabbit HRP	Goat	1:10000	Promega	W4011
Anti-rat HRP	Goat	1:10000	Cell signaling	7077

Next the membrane was incubated with electrochemiluminiscence (ECL) solution (GE Healthcare, USA) for 1 minute in RT. The membrane was then exposed to a film and developed in a dark room on a film.

3.5.2 Protein quantification

Western blot results were quantified using Image J (National Institutes of Health, USA) and Microsoft Excel (Microsoft Corporation, USA). The intensities of each 'protein of interest' band were measured and a graph was plotted in Image J. The areas of the plots were calculated and further analysis was made on Microsoft Excel. The band intensities of the protein of interest were normalized to respective loading control. T-test was performed for

statistical analysis of normalized protein band intensities and a graph was plotted in Prism software (Prism Software, USA). The significance of the results was expressed using a p-value (probability of finding the hypothesis of a study question is significant or not (Dahiru, 2008)). In graph, '*' represents $p \leq 0.05$, '**' represents $p \leq 0.01$ and '***' represents $p \leq 0.001$.

3.6 Immunofluorescence staining

Immunofluorescent staining is a method used to obtain the information about the structure of cell or location of specific molecules within a system. In this method a specific primary antibody (generally monoclonal) is used to attach with a targeted molecule that is being investigated. The primary antibody attachment to the targeted molecule is detected by using secondary antibody. The secondary antibody used in the method is conjugated with fluorescent molecule which can be detected under fluorescent microscope (Donaldson, 2001).

3.6.1 Staining of tissue sections

The colon preserved in OCT was sliced into 6 µm cryosections, using Leica CM3050 S cryostat. The sections were collected in a glass slide and were air dried for 1 hour in RT and then fixed with ice-cold acetone for 10 minutes. The samples were dried after fixation for 1 hour in RT and preserved in -80 ^{o}C until further applications such as immunofluorescent staining.

The tissue sections in the glass slide were encircled using a Dako pen (Dako, China). The Dako pen made the area water repellent, holding the wash/antibodies within the area. It also reduced the amount of chemicals and reagents needed for the sections. The sections were placed in moisture chamber to keep them hydrated. The sections were washed three times, for 5 minutes each, with PBS. After the wash, sections were blocked with buffer A, containing 2.5% BSA (Sigma Aldrich, Germany) for 20 minutes at RT. The sections were re-blocked with buffer B containing 2.5% BSA added with 2% of NGS and 2% of NDS, for 10 minutes at RT. After blocking, the sections were incubated with primary antibody, diluted (table 5) in buffer B. A section of tissue was left with buffer B and was not incubated with primary antibody, as a control for secondary antibody unspecific binding. All samples were incubated with the primary antibody overnight at +4 ^{o}C. The second day of staining was carried out at RT in dark, to avoid any bleaching of fluorescence due to presence of light.

The sections were washed three times with PBS for 5 minutes each and were again blocked with buffer B for 10 minutes. The desired dilution (table 6) of the secondary antibody was prepared in buffer B. The sections were then incubated with secondary antibody for 1 hour at RT in dark. The control section that was not incubated with primary antibody was incubated with secondary antibody. After the secondary incubation, the sections were washed 3 times with 1X PBS for 5 minutes each. The sections were incubated with nuclear dye DRAQ 5 (Cell Signaling), diluted in PBS in the ratio 1:2500, for 5 minutes and washed once with 1X PBS. The sections were then treated with prolong gold mounting media (Sigma Aldrich, Germany) and a cover slip was placed on the top of the sections. The stained samples were left to dry overnight at RT in dark and were preserved at +4 ºC in dark.

Table 5. List of primary antibody used for tissue section immunostaining

Antibody	**Host**	**Concentration**	**Manufacturer**	**Product number**	**Molecular weight (kDa)**
K8 (Troma I)	Rat	1:200	Developmental studies Hybridoma Bank	-	54.1
K20 (IT-Ks20.8)	Mouse	1:200	Progen	AB_531826	48.9
HIF-2a	Rabbit	1:200	Novus biologica	NB 100-122	110

Table 6. List of secondary antibodies used in tissue section staining

Antibody	**Host**	**Concentration**	**Manufacturer**	**Product number**
Anti-mouse Alexa® 568		1:200	Life technologies	A10040
Anti-rabbit Alexa® 488	Donkey	1:200	Life technologies	A21206
Anti-rat Alexa® 568		1:200	Life technologies	A11077
DRAQ5	-	1:12500	Cell signaling	4084S

3.6.2 Staining of CRISPR/Cas9 Caco-2 cells

The cells fixed with 4% PFA on coverslip, were treated with 0.2% nonylphenoxypolyethoxylethanol-40 (NP-40) for 5 minutes at RT. NP-40 permeabilizes the cell membrane for intake of the wash, buffer and antibodies. Similar to the tissue section

staining, the cells were blocked and incubated with buffers (A and B prepared in same way as mentioned in section 4.4.1), primary antibodies (table 7) and secondary antibodies (table 8). The same dilution of DRAQ-5 in tissue section was applied to the cells. Since the cells were on coverslip, prolong gold mounting media was placed on top of the cells in the coverslip. Then the coverslips were mounted over a glass slide and were dried overnight in dark at RT.

Table 7. List of primary antibodies used in cell immunostaining

Antibody	Host	Concentration	Manufacturer	Product number	Molecular weight (kDa)
K8 (Troma I)	Rat	1:1000	Developmental studies HybridomaBank	-	54.1
HIF-1a	Rabbit	1:1000	Novus Biologica	NB 100-134	120

Table 8. List of secondary antibody used in cell immunostaining

Antibody	Host	Concentration	Manufacturer	Product number
Anti-rabbit Alexa® 488	Donkey	1:200	Life technologies	A21206
Anti-rat Alexa® 568	Donkey	1:200	Life technologies	A11077
DRAQ5	-	1:12500	Cell Signalling	4084S

3.7 Transfection of cells

The cell membranes are semi-permeable in nature and play a vital role in exchanging molecules and particles inside and outside the cells (Borrelli et al., 2018). Transfection is a method of introducing DNA construct to the cells to understand the properties of cellular gene and proteins (Kim and Eberwine, 2010). Both chemical and physical methods of transfection were applied to the cells during experiments, in this thesis project.

For chemical method of transfection, lipofectamin 3000 (Thermo Fisher Scientific, USA) was used. Chemical polymers, such as lipofectamin, are cationic lipid or cationic amino acid, interact with amino acid of the plasma membrane to allow DNA plasmid to enter the cell membrane (Kim and Eberwine, 2010). Cells were plated in 35 mm dish with glass bottom

(Mat Tek Corporation, Slovak Republic) and transfected when the confluency was around 30% to 40%, with and without HIF-1a tagged CLIP plasmid (New England Biolabs, England). A mixture of lipofectamin and plasmid was prepared in optimem (Thermo Fisher Scientific, USA) to make the solution serum free and optimize the transfection efficiency. The final concentration of the plasmid was 5µg/ml in the mixture. The cells were incubated with the mixture for 30 minutes and then replaced with fresh medium. The cells were incubated for 48 hours before labeling with CLIP substrate (New England Biolabs, England) and imaging.

A physical method of transfection was applied using Neon electroporation machine (Thermo Fisher Scientific, USA). For the transfection, cells were trypsinized and collected in 50 ml falcon tube. The cell culture medium was added to the cells in falcon tube and prepared a volume of 5 ml. The cell concentration was measured and the tube was centrifuged at 1000 rpm for 4 minutes. The supernatant was removed carefully using suction. The cell suspension buffer of 12 µl was pipetted to the cells in order to plate 800,000 cells /ml. The suspension buffer and cells were mixed well by pipetting up and down gently.

The HIF-1a tagged CLIP plasmid was pipetted to the cell-suspension buffer so that the concentration of plasmid was 5ug/ml. Thus prepared complex of cells, HIF-1a-CLIP plasmid and resuspension buffer was mixed again by pipetting up and down gently. Then the final mixture was pipetted into 10 µl tip, where extra care was given to avoid any bubble into the tip. Then the pipette (containing the mixture in its tip) was placed into the cuvette of the machine filled with 3 ml of electrolyte buffer and electric pulse was applied. For the transfection of HIF-1a CLIP tag plasmid, 1600 V pulse (pulse width of 10 units and 2 consecutive pulses) was applied. The transfected cells were transferred into the cell culture plate and were covered with fresh media (as quickly as possible) and were left for 24 hours for plasmid expression into the cells. For the live cell imaging, special µ-slide angiogenesis well plates (Ibidi, Martimsried Germany) were used. Each well plate (all together 15 wells), were refilled with 50 µl of fresh medium after the transfection.

3.8 SNAP/CLIP labeling

The localization of HIF-1a was observed by labeling the HIF-1a-CLIP tag transfected cells, with CLIP substrate. During the substrate reaction, the CLIP fusion protein tag binds with its consecutive substrate leaving cytosine in the cytoplasm (Gautier et al., 2008).

During the labeling, cells were first washed twice with 1X PBS. A dilution of CLIP substrate (fluorescent label with excitation at 554 nm and emission at 580 nm) was prepared (1:200) in complete DMEM medium. Cells were then incubated with substrate-medium for 30 minutes. The cells were then washed twice with 1X PBS, to remove any non-binding substrate left in the medium. The DNA was counterstained with DRAQ-5 and incubated for 10 minutes (1:10000 in complete DMEM). The cells were again washed once with PBS and topped up with fresh complete DMEM medium. The cells were then directly analyzed with microscopy. Images from 0 hour were taken before adding any chemicals to induce hypoxia. Cells were then treated with 100 µM $CoCl_2$ in complete DMEM medium. Both CRISPR/Cas9 $K8^{+/+}$ and CRISPR/Cas9 $K8^{-/-}$ were labeled at the same time but each was treated with $CoCl_2$ only before microscopy. Imaging of $K8^{-/-}$ cells was performed first to observe HIF-1a nuclear translocation. $K8^{+/+}$ cells were observed after complete imaging of $K8^{-/-}$ cells was done.

3.9 Microscopy and Imaging

Microscopy was an important aspect this thesis project. Different types of microscopes such as bright field, fluorescent and confocal microscope were used to visualize cell growth, confluency and labeled/stained samples. Imaging was carried out using confocal microscopy.

3.9.1 Bright field microscopy

Cells were observed with a Leica DN IL inverted microscope during passaging and growth of the cells. It is a both bright field and phase contrast microscope. The confluency of the cells was observed under 20X and 40X objectives.

3.9.2 Fluorescent and confocal microscopy

An inverted fluorescent microscope was used to determine the success of staining or labeling during the experiments. The microscope used for this purpose was Leica DM IRBE microscope with a mercury light source. Emission filter was selected for respective

wavelength of the fluorophore used for the staining. For e.g., samples stained with Alexa 488 was observed using emission filter of around 500 nm. The cells were observed under 20X objective in the microscope.

When successful staining of the samples was determined, the samples were scanned using Laser scanning confocal Microscope (LCSM). The microscope used in this thesis project was Leica TCS SP5 Matrix. The samples were observed under 20X and oil emersion 63X objective. The images were scanned under 20X for tissues sections and 63X for cell samples. The gain and offset for all comparative samples were adjusted exactly the same for all comparative images while the z-resolution were adjusted where required.

For the live cell imaging with CLIP substrate labeling, Leica TCS SP5 Matrix was used. Before the live cell imaging, the microscope was set to 37 ºC (supplied with 5% CO_2 and humidity) to provide the growth environment to the cells. Upon reaching the suitable environment inside the microscope, the live cell imaging was performed using 20X and oil emersion 40X objective.

3.9.3 Image quantification and statistical analysis

The images obtained from confocal microscopy were analyzed using image J software. Image brightness was adjusted using Leica LAS X software and Image J. Adobe Illustrator and Photoshop were used to prepare an illustrative layout of the results from experiments.

The images obtained from *in vitro* hypoxia experiment were analyzed to observe HIF-1a localization in CRISPR/Cas9 Caco-2 $K8^{+/+}$ and $K8^{-/-}$ cells in normoxia and hypoxia, using Image J. Images were not processed before quantification but brightness was adjusted equally for all comparative images for better analysis. Non-comparative channels (such as DNA) also adjusted for brightens equally in some experiments where images are part of same experiments. In this case, the HIF-1a was observed localized into nucleus in hypoxia in CRISPR/Cas9 $K8^{-/-}$ cells. The level of HIF-1a in nucleus of the both $K8^{+/+}$ and $K8^{-/-}$ cells were quantified by selecting the channel with HIF-1a. The ROI was selected from the nuclear boundaries and HIF-1a mean intensity values were collected from the multiple (nearly 15 per image) nuclear areas (ROIs) of each image, using Image J. The values of each ROI were exported to an excel file and statistical significance was calculated with student t-test. The

same procedure was also applied for the $CoCl_2$ treatment experiment, where HIF-1a intensities were calculated for statistical significance.

4. Results

4.1 Colonocyte keratins, K19 and K20, were up-regulated in hypoxia

Keratins were up-regulated in colon, more specifically K20 (type I) and K7 (type II), when subjected to various type of stress (Helenius et al., 2016). In order to determine if hypoxic stress had a similar influence on keratins in the colon epithelium, mice were subjected to 8% hypoxia. Mice colon samples were collected from normoxia (NOX or control), 4 hours and 24 hours hypoxia (4h HOX and 24h HOX respectively) and keratin levels were analyzed. The up-regulation of HIF-1a *in vivo* (Figure 7A) in hypoxia, compared to normoxia, suggested that the experiment to induce hypoxia worked. In western blot analysis, K19 and K20 were found to be significantly up-regulated under hypoxia compared to normoxia (Figure 7, A-C).

Similar to the hypoxia, the DMOG treatment also up-regulated the HIF-1a level in the mouse colon. K20 was significantly up-regulated with DMOG treatment, while no significant difference in K19 levels was found compared to DMSO treatment (Figure 7, D-F).

The *in vitro* analysis of CRIPSR/Cas9 Caco-2 $K8^{+/+}$ cells also showed similar significant up-regulation of both K19 and K20 during hypoxia (Figure 6, G-H). In contrast to *in vivo* conditions, where K8 levels were unaltered after hypoxia, K8 was also found to be significantly up-regulated *in vitro* in hypoxia compared to normoxia (Figure 7, G-H). The Hsc70 and B-actin (loading control) levels were found to be similar in each sample, suggesting the equal concentration of total proteins of the samples loaded in the gel.

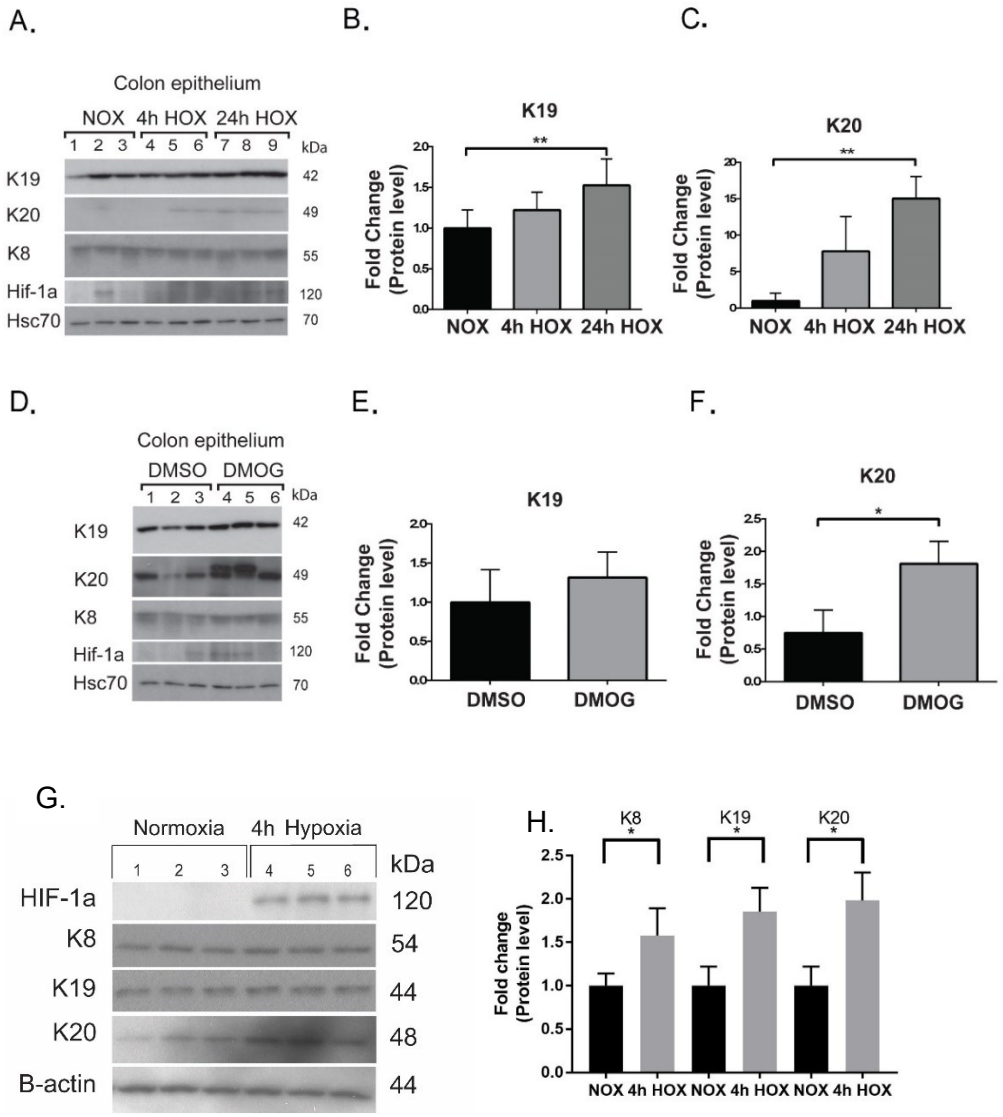

Figure 7. K19 and K20 were up-regulated after 24 hours hypoxia, K20 was up-regulated with DMOG treatment *in vivo* and K8, K19 and K20 were up-regulated *in vitro* after 4 hours hypoxia. Colon tissues of mice from normoxia (NOX), 4 hours hypoxia (4h HOX) and 24 hours hypoxia (24h HOX), supplied with 1% O_2, were collected and homogenized for protein level quantification. (A-F) Samples from the *in vivo* experiment were analyzed for keratins and HIF-1a. **(A)** HIF-1a levels increased in 24 hours hypoxia compared to normoxia. **(A-C)** Colonocyte keratins K19 and K20 were significantly up-regulated in 24 hours hypoxia but the difference was not significant in 4 hours hypoxia. **(D)** Similarly, with DMOG treatment HIF-1a levels were increased compared to DMSO. **(D-F)** K20 was significantly up-regulated with DMOG treatment compared to DMSO treatment but K19 was not significantly different between DMOG and DMSO treatment. **(G-H)** *In vitro* analysis of CRISPR/Cas9 Caco-2 $K8^{+/+}$ cells showed significant up-regulation of K8, K19 and K20 in 4 hours hypoxia compared to normoxia, where HIF-1a levels were highly up-regulated in hypoxia compared to normoxia. Hsc70 (*in vivo*) and B-actin (*in vitro*) were used as loading control. Intensities were balanced to Hsc70 and B-actin intensities respectively. Statistical significance was calculated with student's t-test where * = $p<0.05$, ** = $p<0.01$ and *** = $p<0.001$. n=3.

4.2 K20 crypt localization widened with hypoxia and DMOG treatment compared to controls

In order to determine if K8 and K20 localization were influenced by hypoxia, colon sections were stained with keratins. The colon OCT samples from normoxia and 24 hours hypoxia were sliced into 6 µm sections and fixed with acetone. K8 and K20 were stained to observe if there was altered localization of these keratins after hypoxia compared to normoxia (Figure 8A). The staining result showed increased and slightly widened localization of K20 in the crypt in 24 hours hypoxia compared to normoxia but not K8 (Figure 8A). Similarly, mice colon sections from DMOG and DMSO (control) treatment were prepared in the same way and stained for K8 and K20 (Figure 8B). K20 was found to be localized throughout the colonic crypt after DMOG treatment while it was mostly localized towards crypt top with DMSO treatment (Figure 8A). The K8 localization remained unchanged with DMOG treatment compared to DMSO (Figure 7B).

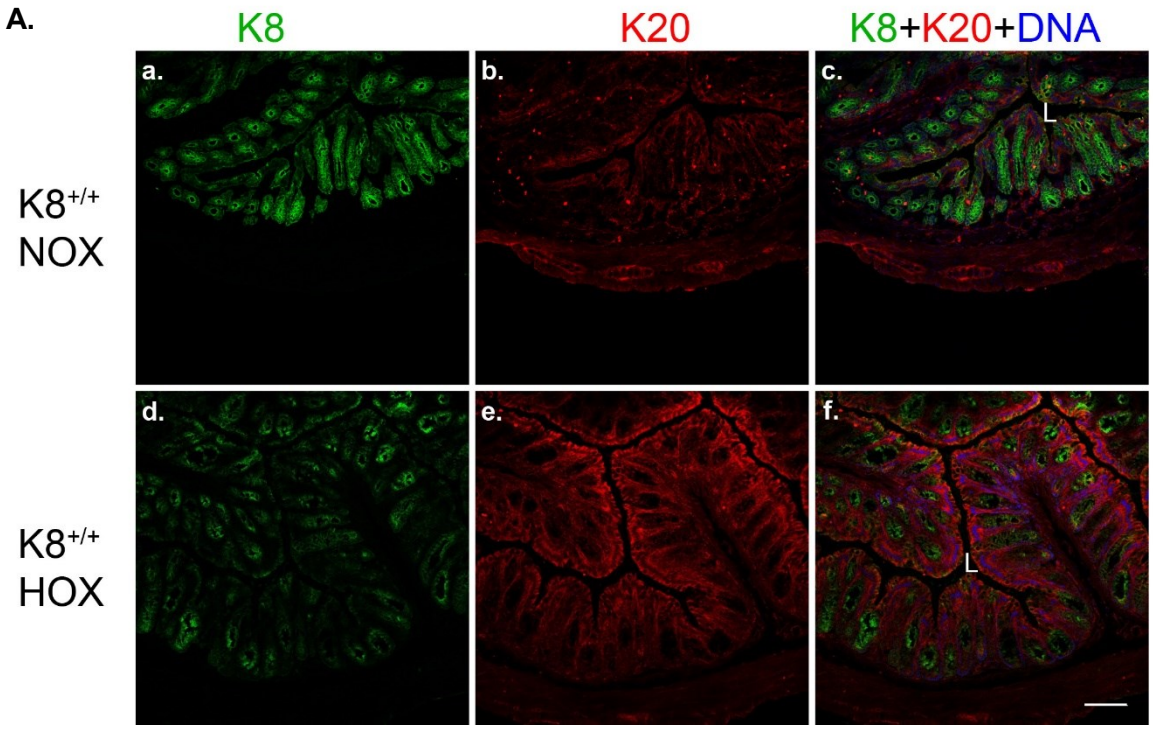

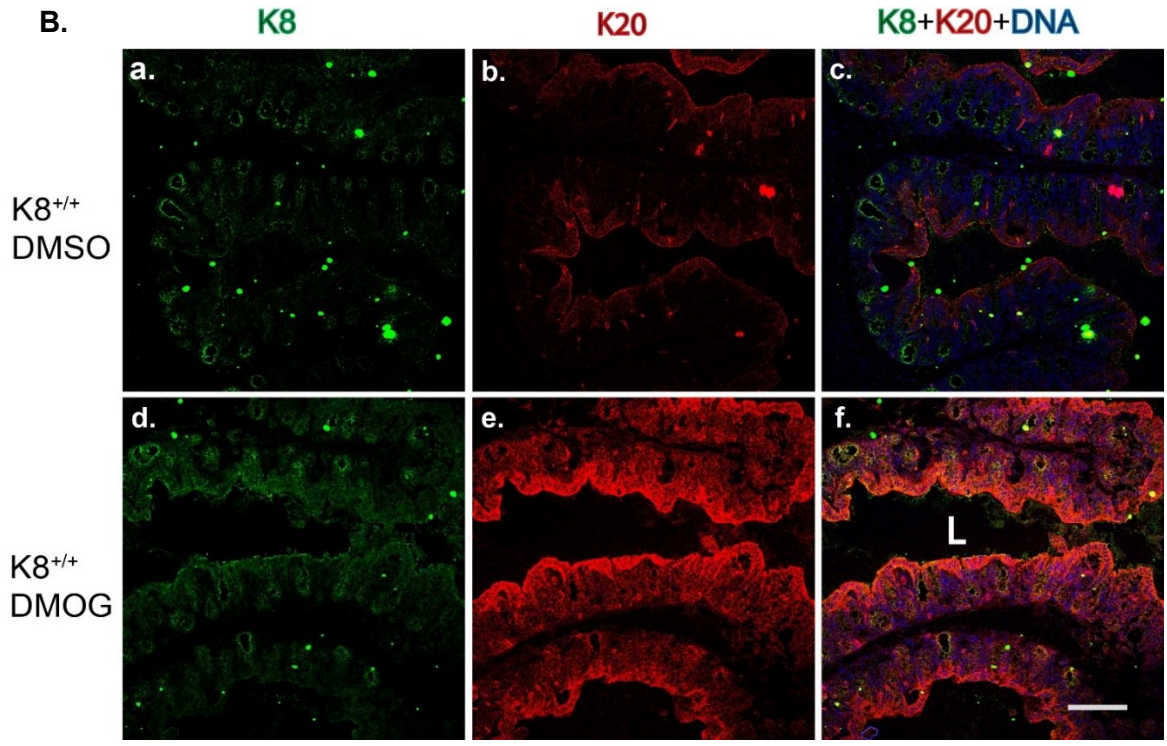

Figure 8. K20 localization was widened in colon crypt after hypoxia and DMOG treatment in K8$^{+/+}$ mice. Colon samples of K8$^{+/+}$ mice from normoxic and hypoxic conditions were cryosectioned into 6 µm slices and fixed with 100% ice cold acetone for 10 minutes. The sections were then stained for K8, K20 and nucleus. The colon epithelium was clearly observed and the keratin staining on the colon epithelium was imaged. **(A)** The localization of K20 was found to be in the top of the colonic crypt in normoxia while it was widened throughout the colonic crypt in hypoxic conditions **(A).** Similarly, the K20 localization was also widened throughout the colonic crypt with DMOG treatment compared to DMSO controls **(B)**. Scale bar is 100 µm and 'L' represents the lumen of the colon. n=3.

4.3 HIFs levels were decreased in mouse colon in the absence of K8

To study whether the absence of K8 led to alterations in HIF levels in colon, samples from K8$^{+/+}$ and K8$^{-/-}$ mice colon were collected and basal levels of HIF-1a and HIF-2a were studied. Analysis of the protein levels showed that both HIF-1a and HIF-2a were down-regulated in K8$^{-/-}$ mice colon compared to K8$^{+/+}$ (Figure 9A). Upon quantification of the western blot result, both HIF-1a and HIF-2a levels were found to be significantly decreased in the K8$^{-/-}$ mice colon compared to K8$^{+/+}$ (Figure 9B). The K8 band (Figure 9A), confirmed the genotype of the mice used, since no signal of K8 was observed in K8$^{-/-}$ mice colon. B-actin was used as loading control, which was observed with similar band intensity for every

sample, in the western blot analysis. The protein levels were normalized to B-actin and statistical significance was calculated with student's t-test.

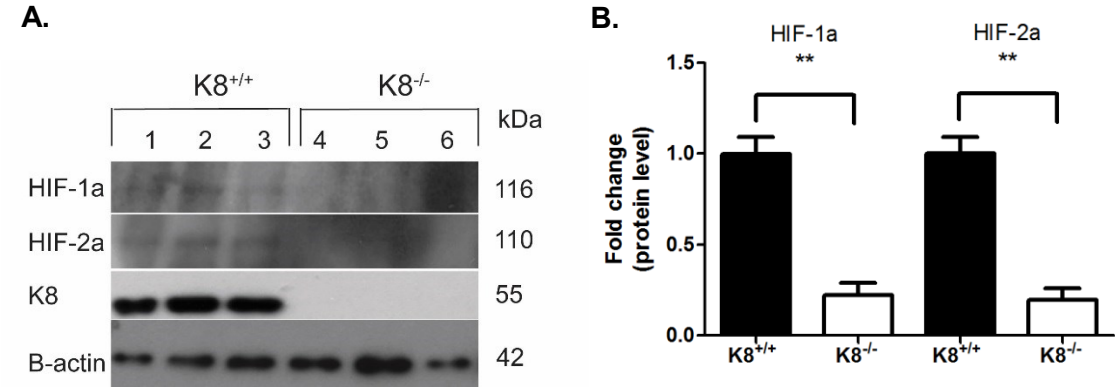

Figure 9. The HIF-1a and HIF-2a levels were decreased in K8$^{-/-}$ mice colon compared to K8$^{+/+}$. The samples were collected from K8$^{+/+}$ (1-3 in Figure 9A) and K8$^{-/-}$ (4-6 in Figure 9A) mice colon and were homogenized for western blot analysis. **(A)** The analysis showed that HIFs levels were decreased in K8$^{-/-}$ mice colon compared to the K8$^{+/+}$ mice colon. **(B)** Quantification of the analysis showed significant decrease in both HIF-1a and HIF-2a levels in K8$^{-/-}$ than in K8$^{+/+}$. B-actin was used as loading control and the HIFs levels were normalized to B-actin levels. Statistical significance was calculated with student's t-test where * = $p<0.05$, ** = $p<0.01$ and *** = $p<0.001$. n=3.

The colon samples were sectioned and stained with HIF-2a and K8 antibody, to observe any alteration of HIF-2a localization caused by loss of K8 in the mice colon (Figure 10). Immunofluorescence staining of the colon section showed similar observation made in protein analysis of HIF-2a levels, where HIF-2a levels were decreased in K8$^{-/-}$ mice colon compared to K8$^{+/+}$ (Figure 9). No difference in localization of HIF-2a was observed in K8$^{-/-}$ colon sections compared to K8$^{+/+}$ mice (Figure 10).

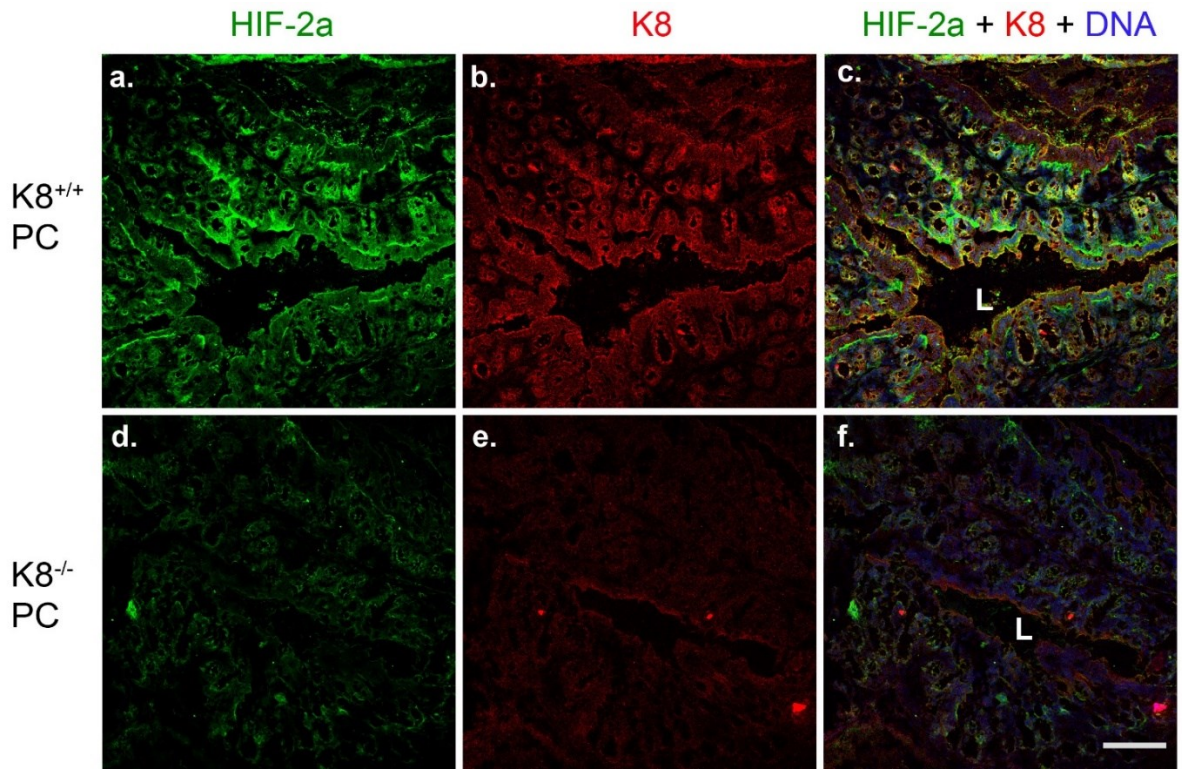

Figure 10. The K8$^{-/-}$ mouse colon had decreased levels of HIF-2a but unaltered localization. The frozen proximal colon (PC) samples in OCT were sliced into 6 µm sections, fixed with ice cold acetone for 10 minutes and were stained for HIF-2a, K8 and the nucleus. The imaging of the immunofluorescence staining confirmed that HIF-2a level was decreased in the K8$^{-/-}$ mice colon compared to the K8$^{+/+}$ mice colon. However, the localization of HIF-2a remained unaltered in K8$^{-/-}$ compared to K8$^{+/+}$. Scale bar = 100 µm and 'L' represents lumen of colon. n=2.

4.4 In CRISPR/Cas9 Caco-2 K8$^{-/-}$ cells, HIF-1a level was increased robustly compared to K8$^{+/+}$ cells

To study whether the presence or absence of K8 affected the levels of HIF-1a and HIF-2a during hypoxia, colon cancer cells with and without K8 were studied. CRISPR/Cas9 Caco-2 K8$^{+/+}$ and CRISPR/Cas9 Caco-2 K8$^{-/-}$ were subjected to hypoxia in a chamber supplied with 1% O_2 (as explained in section 4.2). The samples were collected from normoxia (NOX) and 4 hours hypoxia (4h HOX). The protein analysis of HIF-1a showed up-regulation during hypoxia, where HIF-1a level increased more robustly in the K8$^{-/-}$ cells than in K8$^{+/+}$ cells (Figure 11). The HIF-2a level was also analyzed in K8$^{+/+}$ and K8$^{-/-}$ in both normoxic and hypoxic conditions where no difference was observed (Figure 11).

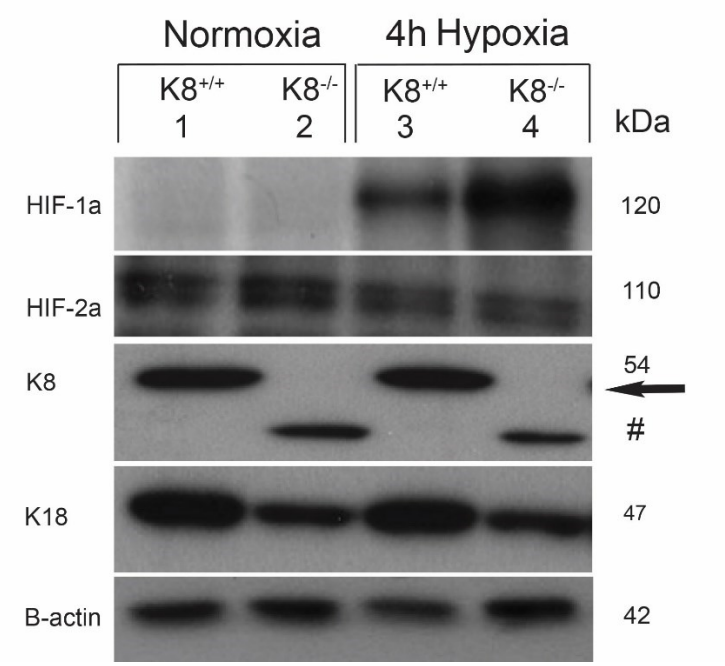

Figure 11. HIF-1a levels were more stabilized in hypoxia in the absence of K8 compared to the cells with K8. CRISPR/Cas9 Caco-2 $K8^{+/+}$ and CRISPR/Cas9 Caco-2 $K8^{-/-}$ cells were subjected to 4 hours hypoxia (1% O_2), samples were collected and homogenized to study different protein levels. Protein analysis for HIF-1a, HIF-2a and keratins (K8 and K18) were performed using western blot method. The western blot analysis showed that the level of HIF-1a was very low in normoxia in both $K8^{+/+}$ and $K8^{-/-}$ cells. HIF-1a level was highly increased in hypoxia in $K8^{-/-}$ cells compared to $K8^{+/+}$ cells. The level of HIF-2a was found to be unchanged in hypoxia compared to normoxia in both $K8^{+/+}$ and $K8^{-/-}$ cells. n=2.

4.5 Absence of K8 induced translocation of HIF-1a in the nucleus

To observe if keratin influenced the localization of HIF-1a, CRISPR/Cas9 Caco-2 $K8^{+/+}$ and $K8^{-/-}$ cells were stained to observe HIF-1a in cells from both normoxic and hypoxic conditions. Immunofluorescent staining of HIF-1a revealed that HIF-1a was mostly present in the cytoplasm in normoxia, in both $K8^{+/+}$ and $K8^{-/-}$ cells (Figure 12). No difference in the HIF-1a levels and localization were observed in normoxia between CRISPR/Cas9 Caco-2 $K8^{+/+}$ cells and CRISPR/Cas9 Caco-2 $K8^{-/-}$ cells. Cells treated for 4 hours in hypoxic conditions had increased intensity of the HIF-1a in CRISPR/Cas9 Caco-2 $K8^{+/+}$ compared to normoxia and the increase was even higher in CRISPR/Cas9 Caco-2 $K8^{-/-}$ cells, which verified the western blot data. HIF-1a translocated to the nucleus in CRISPR/Cas9 Caco-2 $K8^{-/-}$ cells and the HIF-1a intensity was significantly higher in the nucleus of $K8^{-/-}$ cells compared to CRISPR/Cas9 Caco-2 $K8^{+/+}$, when subjected to 4 hours hypoxia (Figure 12).

In order to confirm the genotype, CRISPR/Cas9 Caco-2 cells were stained with K8 along with HIF-1a under both hypoxic and normoxic conditions. Keratins were observed as filaments in CRISPR/Cas9 Caco-2 $K8^{+/+}$ cells (Figure 12). In CRISPR/Cas9 Caco-2 $K8^{-/-}$ cells, dots like structure were observed in the same channel as K8 is observed, in both normoxia and hypoxia (Figure 12). The western blot analysis of K8 with same antibody also showed a lower band in CRISPR/Cas9 Caco-2 $K8^{-/-}$ cells (represented by '#' in Figure 11) which concordance the data from the staining results.

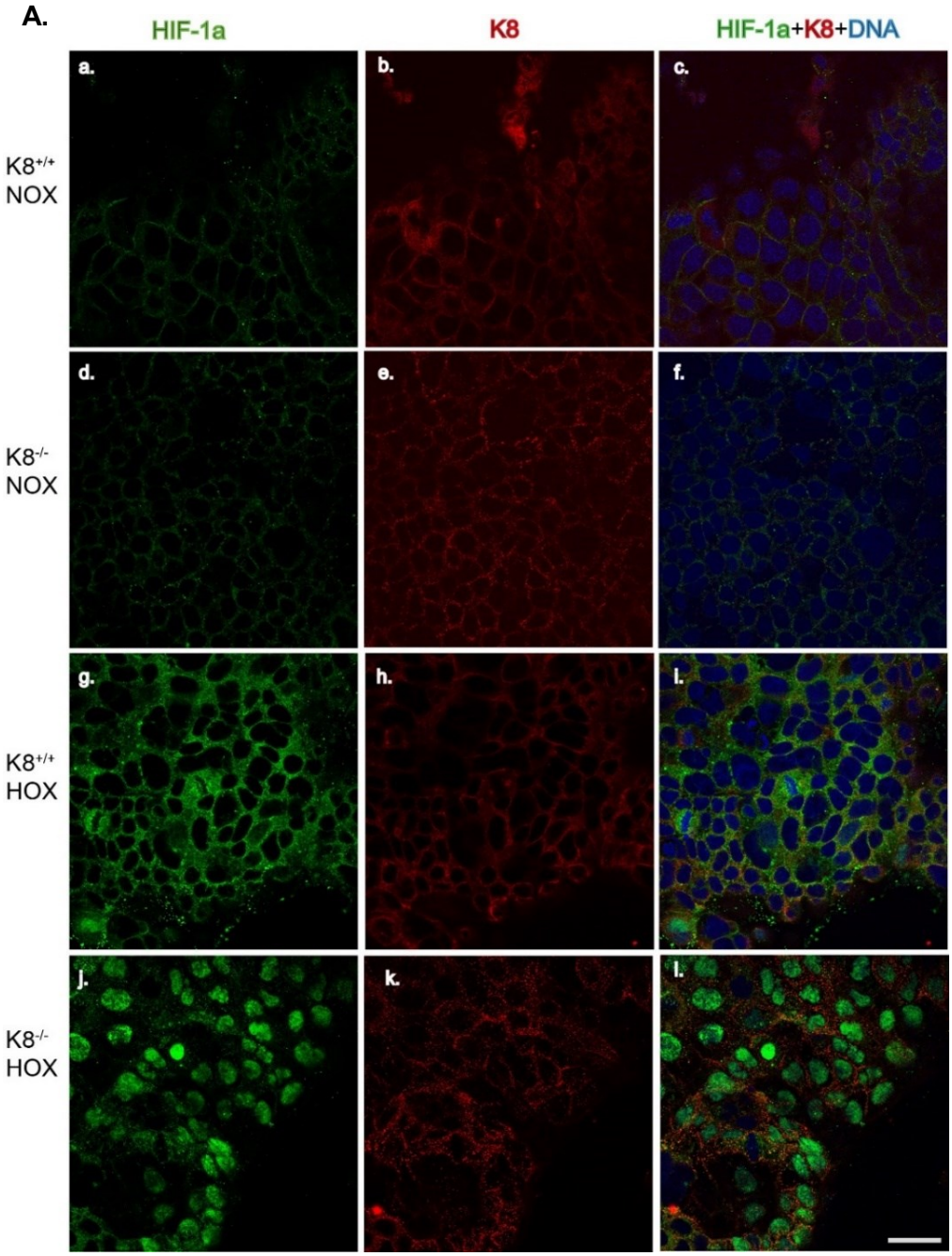

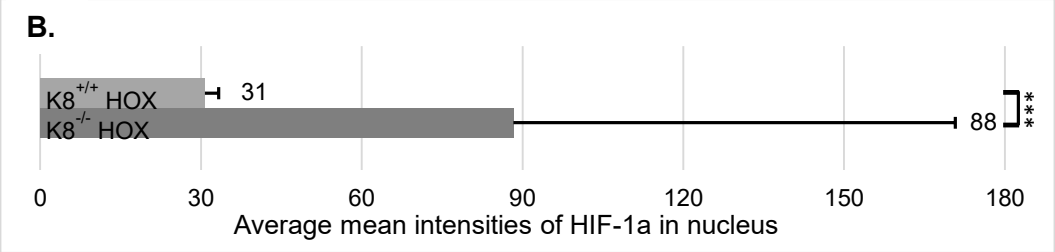

Figure 12. HIF-1a was translocated to the nucleus in absence of K8, in hypoxic conditions. CRISPR/Cas9 Caco-2 $K8^{+/+}$ and $K8^{-/-}$ cells were grown in glass coverslip and subjected to the hypoxia (1% O_2) for 4 hours. The cells were stained with HIF-1a, K8 and nucleus from both normoxic and hypoxic conditions. **(A)** The nuclear translocations of HIF-1a, from the cytoplasm to the nucleus, was observed in hypoxic conditions compared to normoxic conditions. The nuclear translocations were even more in $K8^{-/-}$ cells compared to $K8^{+/+}$ cells, in hypoxia. **(B)** When quantified, a significant difference in location of HIF-1a in nucleus, between $K8^{-/-}$ and $K8^{+/+}$ was found in hypoxia, with higher HIF-1a nuclear localization in $k8^{-/-}$ cells compared to $K8^{+/+}$ cells. The levels of nuclear HIF-1 were measured by measuring the signal intensity, using Image J (Appendices 1) and quantified using student t-test analysis. There were no nuclear translocation of HIF-1a, in normoxic condition, observed in both $K8^{+/+}$ and $K8^{-/-}$ cells. Statistical significance was calculated with students t-test where * = $p<0.05$, ** = $p<0.01$ and *** = $p<0.001$. Scale bar was 50 µm.

4.6 HIF-1a was up-regulated with $CoCl_2$ treatment and translocated more efficiently to the nucleus in absence of K8 compared to the cells with K8

$CoCl_2$ is a chemical compound that mimics hypoxia and stabilizes HIF-1a (Yuan et al., 2003), therefore, it was used in the *in vitro* assessment of this project. In order to investigate if absence of K8 led to up-regulation and nuclear translocation of HIF-1a with $CoCl_2$ treatment, CRISPR/Cas9 Caco-2 $K8^{+/+}$ and $K8^{-/-}$ cells were treated with 400 µM $CoCl_2$ for 4 hours. Both CRIPSR/Cas9 Caco-2 $K8^{+/+}$ and CRIPSR/Cas9 Caco-2 $K8^{-/-}$ were chemically treated at the same time and samples were homogenized for protein analysis. Western blot analysis showed that the HIF-1a levels were increased after treating cells with 400 µM $CoCl_2$ for 4 hours (Figure 13A), similar to hypoxia experiment where HIF-1a levels increased after 4 hours of hypoxia treatment to the cells (Figure11). Likewise, HIF-1a levels increased even higher in $K8^{-/-}$ cells compared to $K8^{+/+}$ cells, which was consistent with the results of hypoxic treatment to the cells.

HIF-1a was up-regulated and translocated to the nucleus more significantly in CRISPR/Cas9 Caco-2 $K8^{-/-}$ cells compared to $K8^{+/+}$ cells, when subjected to 4 hours hypoxia (Figure 12).

Similar observation was made with 400 µM $CoCl_2$ treatment for 4 hours to the cells. HIF-1a was up-regulated and translocated to the nucleus after the treatment (Figure 13B). The intensity of HIF-1a staining was quantified by calculating mean intensity in the nucleus of the cells, where significant increase in HIF-1a level was observed in $K8^{-/-}$ cells compared to $K8^{+/+}$ cells, after treating cells for 4 hours with 400 µM $CoCl_2$ (Figure 13C). Scale bar 50 µm.

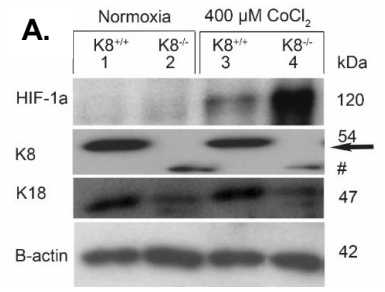

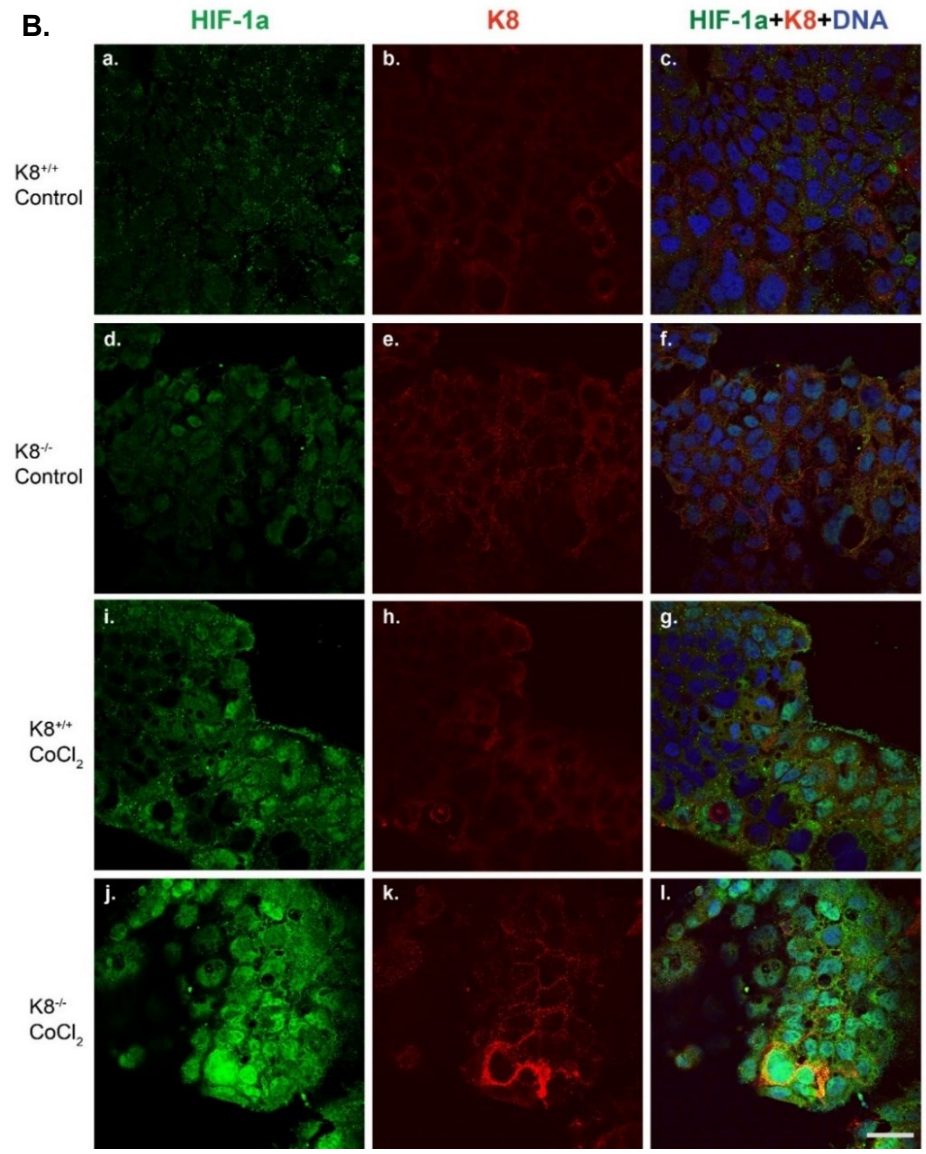

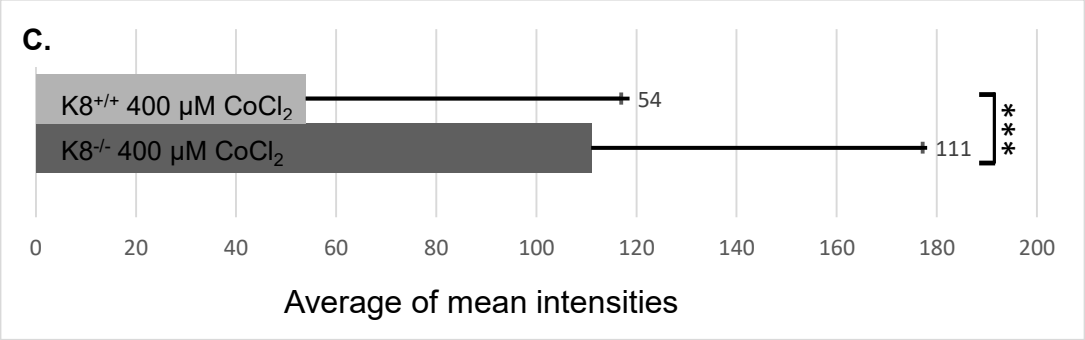

Figure 13. $CoCl_2$ treatment increased HIF-1a levels mostly in $K8^{-/-}$ cells and induced the nuclear translocation of HIF-1a in $K8^{-/-}$ cells. The cells were treated with 400 µM $CoCl_2$ for 4 hours. **(A)** The HIF-1a levels was highly up-regulated in the cells that were treated with $CoCl_2$ compared to the cells in normoxia. The up-regulation of HIF-1a was higher in $K8^{-/-}$ cells treated with 400 µM $CoCl_2$, compared to the $K8^{+/+}$ cells treated with same concentration of $CoCl_2$. **(B)** Immunofluorescent staining of HIF-1a and K8, showed that the HIF-1a translocated to the nucleus when treated with 400 µM $CoCl_2$ for 4 hours. **(C)** When quantified, the intensity of HIF-1a in the nucleus of $K8^{-/-}$ cells was significantly higher compared to $K8^{+/+}$ cells, both treated with 400µM $CoCl_2$. In figure, scale bar represents 50 µm length and statistical significance was calculated with students t-test where * = $p<0.05$, ** = $p<0.01$ and *** = $p<0.001$. n=2.

4.7 Pilot experiment for live cell imaging with SNAP/CLIP tag novel labeling technique

Live cell imaging of CRIPSR/Cas9 Caco-2 cells was performed to determine the exact time of nuclear localization of HIF-1a, by transfecting cells with HIF-1a tagged CLIP plasmid, then labeling with CLIP substrate and treating the cells with 100 µM $CoCl_2$. Both CRISPR/Cas9 Caco-2 $K8^{+/+}$ and CRISPR/Cas9 Caco-2 $K8^{-/-}$ were transfected and labeled at the same time. Live cell imaging showed that a low signal of HIF-1a was present mostly in the cytoplasm of the $K8^{-/-}$ cells and extremely low in the nucleus of the cells, in normoxia (0 minute). As shown in figure (Figure 14), at each interval of 10 minutes, the HIF-1a fluorescence intensity signal was gradually decreased over 70 minutes time, likely due to bleaching, when the same area of the cell plate was observed. At 70 minutes, when other areas of the cell plate (represented by * in figure 14) were observed, increase in HIF-1a signal was observed in the nucleus of the cells compared to the 0 minute fluorescence intensity (*) (Figure 14). However, this pilot experiment was not very conclusive data due to various factors which are explained in the discussion section 5.3.

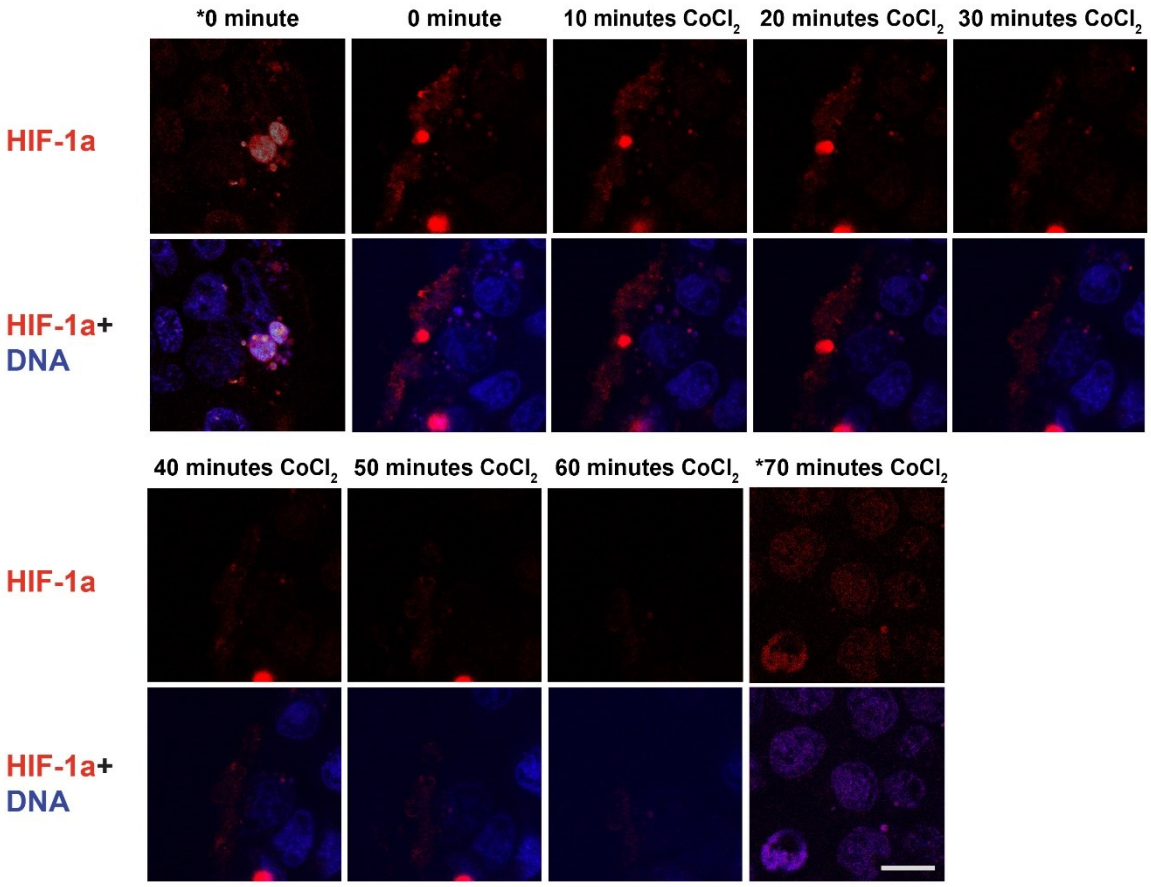

Figure 14. Live cell imaging of nuclear translocation of HIF-1a using CLIP tag labeling method. The cells were chemically transfected with HIF-1a attached CLIP tag plasmid. The cells were labeled with CLIP substrate of excitation wavelength 553 nm. The images were taken at 0 minute (control) from different areas of the cells (represented by * in the figure). The cells were then treated with 400 µM $CoCl_2$ and consecutive images from same area were taken at the interval of 10 minutes each. The comparative observation of cells from different areas (*) at 0 minute and 70 minutes showed possible nuclear translocation of HIF-1a within 70 minutes of the 400µM CoCl2 treatment in the $K8^{-/-}$ cells.

4.8 CRISPR/Cas9 Caco-2 $K8^{-/-}$ cells had low level of keratins in higher passage compared to lower passage cells

In order to determine if the analysis of keratins and HIF proteins can be studied in a cell line regardless the passage number of cell, keratin levels from different passages of the CRISPR Caco-2 cells were studied from both $K8^{+/+}$ (high passage P24 and low passage P10) and $K8^{-/-}$ (high passage P22 and low passage P8) cells. Passaging cells for longer time showed decrease in keratin levels in $K8^{-/-}$ cells. Both type I (K18, K19 and K20) and type II keratin (K7) were found to be significantly decreased in P22 $K8^{-/-}$ cells compared to P8 cells (Figure

15). However, no change in keratin levels was detected in $K8^{+/+}$ between high and low passages of cells (Figure 15A). Similarly, the HIF-1a level was also analyzed and no difference in HIF-1a level was observed between $K8^{+/+}$ and $K8^{-/-}$ cells (Figure 15A).

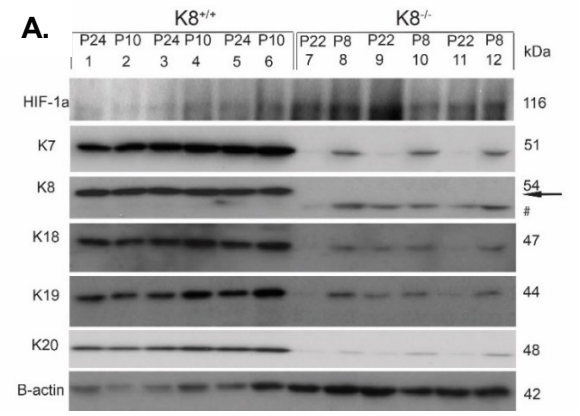

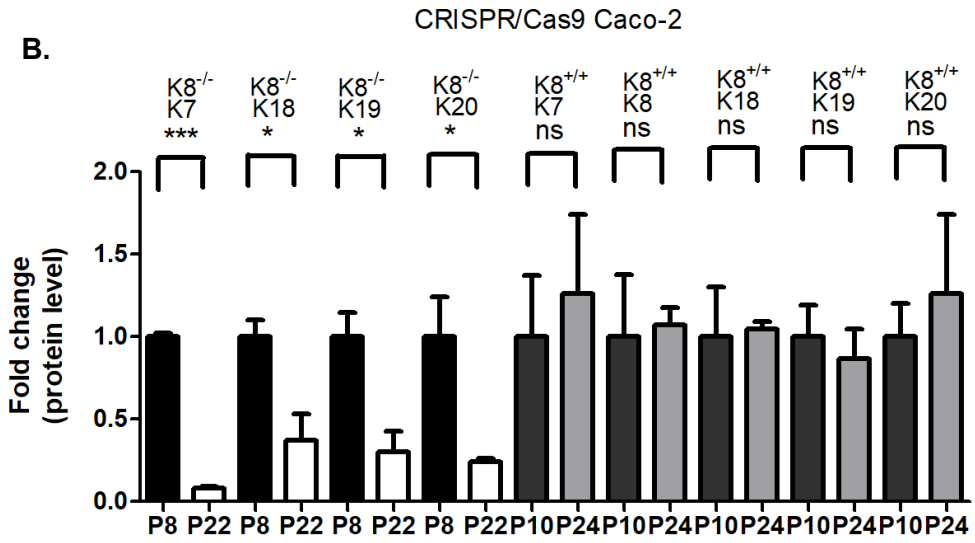

Figure 15. Figure 15. CRISPR/Cas9 Caco-2 $K8^{-/-}$ cells had remnant keratin levels when cultured long time. CRISPR/Cas9 Caco-2 $K8^{+/+}$ and CRISPR/Cas9 Caco-2 $K8^{-/-}$ cells were grown from passage 10 (P10) and passage 8 (P8) respectively. Cell samples were collected when they were P10 ($K8^{+/+}$) and P8 ($K8^{-/-}$) and reached passage 24 (P24) of $K8^{+/+}$ and passage 22 (P22) of $K8^{-/-}$. Samples were homogenized and protein concentrations of each sample were determined. **(A)** Immunoblotting was performed for HIF-1a, type I keratins (K18, K19 and K20) and type II keratins (K7 and K8). The immunoblotting of HIF-1a showed no difference in protein levels between $K8^{+/+}$ and $K8^{-/-}$ cells regardless the passage number. Likewise, both type I and type II keratin levels were similar in $K8^{+/+}$ between P24 and P10. **(B)** Interestingly, both type I (K18, K19 and K20) and type II keratins (K7) were found to be significantly decreased in P22 of $K8^{-/-}$ cells compared to P8 of $K8^{-/-}$ cells. B-actin was used as loading control and protein levels were normalized to B-actin. In figure 15 (A), 1-6 indicates $K8^{+/+}$ cells while 7-12 indicates $K8^{-/-}$ cells. Statistical significance was calculated with students t-test where * = $p<0.05$, ** = $p<0.01$ and *** = $p<0.001$. n=1.

4.9 HIF-1a levels were decreased in CRISPR/Cas9 Caco-2 cells when incubated with same culture medium for 72 hours

During analysis of other experiments in this project, we observed that HIF-1a level were altered depending on the incubation duration with the same (initial) medium. In order to verify our observations that HIF-1a level may had altered between cells with fresh medium and cells with old medium, CRISPR/Cas9 $K8^{+/+}$ and $K8^{-/-}$ cells were seeded and incubated with the same culture medium for 72 hours (initial medium) and samples were collected. Cells were also washed and incubated with fresh medium for 2 hours, after 72 hours incubation with the initial medium and samples were collected. In western blot analysis, it was observed that cells with initial medium incubated for 72 hours had higher levels of HIF-1a compared to the cells incubated with fresh medium for 2 hours more. The level of HIF-1a was likely increased in $K8^{-/-}$ cells compared $K8^{+/+}$ cells but upon quantification no significant difference was found (Figure 16). B-actin was used as loading control which was found to be evenly present in each sample.

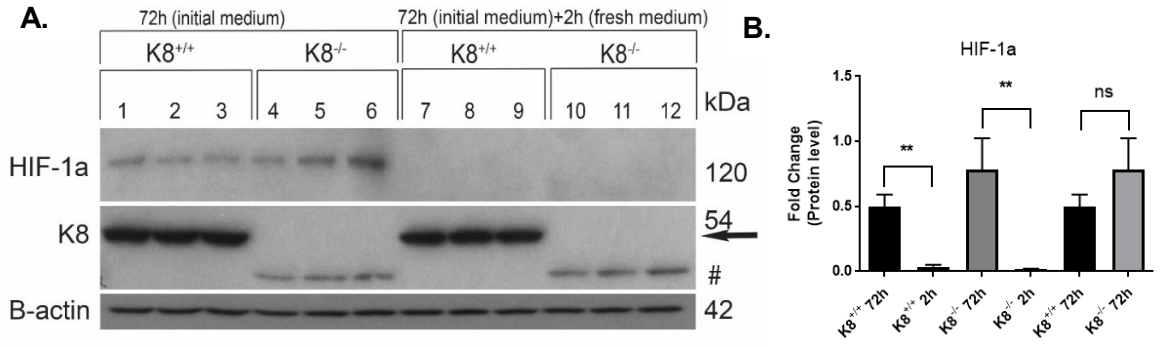

Figure 16. HIF-1a levels were increased in CRISPR/Cas9 Caco-2 cells when they were grown with initial medium for 72 hours. Both CRISPR/Cas9 Caco-2 $K8^{+/+}$ and $K8^{-/-}$ cells were grown with the same culture medium for 72 hours. The cells from both $K8^{+/+}$ and $K8^{-/-}$ were lysed in homogenization buffer after 72 hours without changing the medium (initial medium). Cells were also washed and incubated with fresh medium for 2 hours more and cells were homogenized for further analysis. **(A)** HIF-1a levels were analyzed using western blot method and **(B)** statistical quantification showed that HIF-1a levels were significantly increased in the cells incubated with initial medium for 72 hours compared to the cells incubated for 2 hours more with fresh medium in both $K8^{+/+}$ and $K8^{-/-}$ cells. No significant difference was observed in the HIF-1a level between $K8^{+/+}$ and $K8^{-/-}$ cells incubated for 72 hours with initial medium (p=0.12). B-actin was used as loading control. Statistical significance was calculated with students t-test where * = $p<0.05$, ** = $p<0.01$ and *** = $p<0.001$. n=1.

5. Discussion

Hypoxia is characterized by an increased level of HIF-1 transcription factors: HIF-1a, HIF-2a and HIF-3a. HIF-1a along with its heterodimer HIF-1b are responsible for transcription of the vascular endothelial growth factor (VEGF) and is very important in the embryonic stage of the cell for growth and development. Normal expression of HIFs is essential for maintaining the oxygen level in cells, while over expression of HIF-1a is associated with cancer cell angiogenesis, proliferation and growth of tumor (Elson et al., 2001; Stoeltzing et al., 2004). Deactivation of HIF-1a has been shown to inhibit the growth and angiogenesis of gastric tumors, pancreatic tumors and hepatic cells (Stoeltzing et al., 2004).

Stress in colonic epithelium promotes up-regulation of keratins, where keratins act as a protector against stress (Asghar et al., 2015; Helenius et al., 2016). This thesis project was carried out to understand more about colon epithelial keratins under stress, such as hypoxia. There is evidence that hypoxic stress can change the structure of the epithelial cytoskeleton in alveolar cells, where K8 and K18 are found to be degraded under hypoxic stress (Na et al., 2010). Therefore, we hypothesized that keratins play an important role in hypoxia signaling and may respond to hypoxia in a similar way as stress to protect cells from hypoxic stress in the colonic epithelium. While HIF factors are important in adapting the low O_2 and promoting the development of cancer cells by triggering HIF-dependent pathways, keratins are the defenders against the hypoxic stress. If keratins are the major protectors and defenders against mechanical, chemical or hypoxic stress to the cells, they could be the important proteins to defend against cancer as well. Further study is needed on the role of keratins in hypoxia and the mechanism behind regulation of keratins in hypoxia.

5.1 Keratins are stress protectors and respond to hypoxic stress

It has been pointed out by Toivola and co-workers in 2015 (Toivola et al., 2015) that keratins are stress protectors. Also, the up-regulation of keratins in intestinal stress, shown by Helenius and co-workers, 2016 (Helenius et al., 2016), follow the concept of keratins as stress protectors. Moreover, the study by Na et al in 2010 has stated that keratins respond to hypoxia as stress factor by down-regulating keratins in hypoxia in alveolar epithelial cells, thereby connecting the link between epithelial keratins and hypoxia. Based on these concepts, the data established in Figure 7 (A-D), where K19 and K20 were up-regulated in hypoxia and

DMOG treatment compared to normoxia, suggested that K19 and K20, indeed respond to hypoxia as a stress factor and generates stress to the cells. Similar to this *in vivo* data (Figure 7, A-D), the *in vitro* analysis of CRISPR/Cas9 Caco-2 $K8^{+/+}$ also showed up-regulation of keratins after 4 hours of hypoxia (Figure 7, D-E). The extremely low levels of HIFs (HIF-1a and HIF-2a) in the absence of K8 (Figure 9, A-B) also suggested that there is already a link between keratins and HIFs and keratins determine the level of HIFs in the colonic epithelium under basal condition.

5.1.1 Absence of K8 reduces the beneficiary function of HIF-1a and down-regulates HIF-2a in colon under normoxic condition

HIF-1a is known to have a protective role in IBD (Shah, 2016). HIF-1a activation also leads to formation of β-defensins (anti-microbial protein) and decrease of cytokines in IBD (Shah, 2016). Similarly, HIF-2a have a proliferative and regenerative role in IBD. Moderate activation of HIF-2a is not harmful to the epithelium, while overexpression of HIF-2a leads to colitis (Shah, 2016). It has also been shown that mice with absence of K8 have colitis in their colon and are more susceptible to colon cancer (Asghar et al., 2015; Baribault et al., 1993; Liu et al., 2017). Similar to the facts stated, the results (Figure 9) showed a correlation between keratins and HIFs in colon where the lack of keratin in colon epithelium correlated with the expression of HIF-1a and HIF-2a. The lack of keratins in $K8^{-/-}$ mice colon could be inhibiting the formation of HIF proteins in colon and further promoted IBD and CRC formation in colon (Misiorek, 2016). In addition, absence of K8 leads to diarrhea in $K8^{-/-}$ mice and their colon epithelium has significantly longer crypt due to hyper proliferation compared to $K8^{+/+}$ mice (Asghar et al., 2015). Although HIF-2a is regenerative in function and up-regulated in cancer, the down-regulation of HIF-2a in $K8^{-/-}$ mice made it difficult to understand the role of K8 in HIF-2a regulation in $K8^{-/-}$ colonic epithelium. It has to be studied in depth how and why keratins are regulating HIFs levels, but from the results (Figure 7 and Figure 9) where keratins were up-regulated and prevented translocation of HIF-1a from cytoplasm to nucleus in hypoxia, it could be concluded that the functions of HIFs are dependent upon the amount of K8 present in the cells. Furthermore, the up-regulation of HIF-1a and keratins (K19 and K20) in hypoxic conditions (Figure 7) justified the link between keratins and HIFs and a potential role of keratins in regulation for HIFs factors and the hypoxia signaling pathway.

5.2 K8 regulates the nuclear translocation HIF-1a during hypoxia

Nuclear translocation of HIF-1a has been linked with nuclear transporters such as importin, resulting in the activation of target genes such as VEGF, epo and glut-1 but complete mechanism of the translocation is not fully understood (Depping et al., 2008). It has also been reported that the translocation is independent of O_2 levels and more dependent of the stabilization of HIF proteins (Luo and Shibuya, 2001). Our study, where the absence of K8 in CRISPR/Cas9 Caco-2 $K8^{-/-}$, showed increased nuclear translocation of HIF-1a, could be an indication that keratins are the mediator of HIFs transport to the nucleus. There were low levels of HIF-1a in normoxia in both CRISPR/Cas9 Caco-2 $K8^{+/+}$ and CRISPR/Cas9 Caco-2 $K8^{-/-}$ cells compared to these cells in hypoxia (Figure 11). This suggests that the presence of K8 in cells affects the cytoplasmic accumulation of HIF-1a while the absence of K8 results in more efficient nuclear translocation of HIF-1a. However, preliminary results from Toivola lab, shows that absence of K8 also results in down-regulation of nuclear lamins (proteins found in the nuclear membrane). Down-regulation of lamins in nuclear membrane makes the membrane loose and more permeable, which might open up the channel to the HIF-1a for more efficient nuclear translocation (Stenvall, Nyström et al; unpublished data). However, a time course hypoxia treatment to the cells can be performed to check if it is possible for $K8^{+/+}$ cells to peak the HIF-1a levels already before 4 hours and if it is only a slower mechanism in $K8^{-/-}$ cells that the HIF-1a level peaks at around 4 hours.

5.3 Live cell imaging of a degrading protein: a challenge

Many years have passed after the introduction of live cell imaging. It is hard to deny that molecular biology has been changed ever since. Optimization of microscopy and tools are always being developed to overcome the challenges that live cell imaging bears. In spite of different progresses in the field, it is still challenging to perform live cell imaging due to limitation possessed by certain properties such as real time study of cellular property (adhesiveness and changes due to environmental factors) and fluorescent properties of molecular probes (Cole, 2014) . In this master's thesis, live cell imaging was performed to investigate the real time-point of the nuclear translocation of HIF-1a using 100 µM $CoCl_2$. It was a pilot experiment, performed first time in the lab, by self-generating the protocol and procedure. During imaging, CRISPR/Cas9 Caco-2 $K8^{-/-}$ cells were observed first, since the hypoxia induced nuclear translocations of HIF-1a were mostly observed in CRISPR/Cas9

Caco-2 $K8^{-/-}$ cells (Figure 12). Although the experiment was partially successful, there were many challenges faced during the experiment. HIF-1a is a degradable transcriptional factors, hydoxylated by PHDs, in normoxia (Dengler et al., 2014; Eales et al., 2016). Likely because the imaging was performed after 48 hours of chemical transfection of HIF-1a, an extremely low signal in HIF-1a/red channel was observed, even during the first observation in the microscope. It was very difficult to differentiate the actual signal from noise or background because the fluorescence signal overall was very low. It also affected observation of single cell in higher magnification, since there was not enough signal present in the cells. Moreover, there was difficulty in observing the same spot on the cell plate during whole observation time due to the movement of the cells (Figure 14). Although it was difficult to say if the observed signal was obtained from the protein of interest, the experiment was carried out. Overtime, the cells were moving away from the focal point, which can be also seen in Figure 14. Since there was no possibility of obtaining signal from the cells in the spot due to movement or bleaching of the substrate, another area was viewed. There were more signal observed inside the nucleus in 70 minutes of the $CoCl_2$ treatment, compared to 0 minute, in the different areas (marked by * in figure 14). Since HIF-1a was the only protein labeled, the observed signal was believed to be from the same protein. However the imaging was performed only once, the data from this results needs to be verified and remains inconclusive at this stage. The images (Figure 14) were obtained increasing the brightness (only) by three folds from the original data and no other image processing was performed.

5.3.1 Increased transfection efficiency resulted in better observation of the live cell imaging

The poor CLIP-HIF-1a signal seen in live cell imaging was likely due to low HIF-1a signal present. Therefore, a new way of transfection was carried out using Neon transfection system (explained in section 3.7), which increased the transfection efficiency (Figure 17). The cells were observed under microscope after 24 hours of transfection to prevent degradation of HIF-1a as much as possible. The angiogenesis cell plates from Ibidi were used in order to optimize cell amount and substrate amount (50 µl per well). It also improved cell recovery after the transfection within short period of time. Although there was improved fluorescence signal in both CRISPR/Cas9 Caco-2 $K8^{+/+}$ and CRISPR/Cas9 Caco-2 $K8^{-/-}$ cells (Figure 17), the imaging was not performed due to complications faced in microscope (such as difficult to

focus). However, it was hard to understand whether the problem was due to cell plate, medium or microscope itself (Cole, 2014). Further experiment needs to be carried out to investigate the exact time point of the nuclear translocation of HIF-1a.

5.4 Changes in cellular mechanism observed due to long passaging and nutrition

Studies have shown that there are differences in cellular behavior such as cell differentiation, senescence and cell attachment, from donor to donor and also between the cell passages from the same cell line (Kretlow et al., 2008). Similar observations were made in cellular behavior of CRISPR/cas9 Caco-2 cell line between different passages of the cells. The samples were collected from both $K8^{+/+}$ and $K8^{-/-}$ cells at passage 10 and passage 8 for $K8^{+/+}$ and $K8^{-/-}$ respectively, (considered as low passage), and passage 24 and passage 22 again for both $K8^{+/+}$ and $K8^{-/-}$ cells respectively, (considered as high passage). The western blot analysis and quantification of keratin levels showed that significantly lower levels of keratins present in higher passage $K8^{-/-}$ cells compared to lower passage $K8^{-/-}$ cells (Figure 15). Likewise, there was always observed an extra band (molecular weight nearly 42 kDa) when immunoblotting the samples from $K8^{-/-}$ cells, using theK8 antibody (Troma I) (as represented by '#' in the figures in result section: Figure 11 and Figure 13). Yet, we have not identified the band, if it is a degraded form of K8 or any other type of keratin/some other proteins detected by Troma I (K8) antibody. It is also consistent with the staining of the $K8^{-/-}$ cells where dotted cytoplasmic structures (not filament) were seen (Figure 12 and Figure 13) in the same channel stained for K8 using K8 (Troma I) antibody (PFA fixation).

Besides passaging, the change of cell culture medium influenced some protein levels in the cells. To understand if medium had any effect on the cells, samples from CRISPR/Cas9 $K8^{+/+}$ and CRISPR/Cas9 $K8^{-/-}$ cells were collected after incubating cells with initial medium for 72 hours and again incubating cells with medium for 2 hours. In figure 15, there was seen an impact on HIF-1a levels in the cells due to fresh medium. When incubated with the initial medium for 72 hours, the HIF-1a levels were significantly high in both $K8^{+/+}$ and $K8^{-/-}$ cells compared to the cells incubated with fresh medium for 2 hours more. A likely higher level of HIF-1a in $K8^{-/-}$ cells, incubated with initial medium, was observed compare to $K8^{+/+}$ cells but no significant difference was observed. The expression of HIF-1a level in the samples from the cells incubated with initial medium only, suggested that HIF-1a up-regulation or the activation could be regulated by the nutritional factors. In other words, the consumption of

nutrients in the initial medium may have provided stress to the cells there by activating the hypoxia signaling pathway. Since colonic epithelium has low amount of oxygen, there might be low nutrition supply. Some studies shows, HIF-1a is linked with adipose tissue O_2 deficiency in obese animals (Lee et al., 2014). The oxygen consumption in high fat diet (HFD) mice is higher than in normal lean mice and increased level of HIF-1a mRNA and protein levels are seen in HFD mice. Mice which are overexpressing adipocyte-specific HIF-1a further develop adipose tissue inflammation and insulin resistance (Lee et al., 2014). It has also been reported before that the medium change effects on cell growth, verified long ago (Griffiths, 1971). However, *in vitro* study of HIFs protein regulation due to consumption of medium may not been reported until now. During this project, not enough study was performed to verify the HIFs regulation with nutrient consumption. This needs more study, both *in vivo* and *in vitro,* in order to verify a possible link between the metabolism and HIF-1a activation.

6. Conclusion

The results of this thesis show that keratins are up-regulated in hypoxic stress and protect cells against hypoxic stress in colonic epithelium. Keratins also determine the level of HIFs in colon cancer cells and modulate the regulation of oxygen-dependent molecules and HIFs signaling. Keratin, specifically K8, plays a role in translocation of HIF-1a in hypoxic condition. In absence of K8, HIF-1a translocate to the nucleus in hypoxia, suggesting K8 plays a major role in preventing overexpression of HIF-1a and gene transcription.

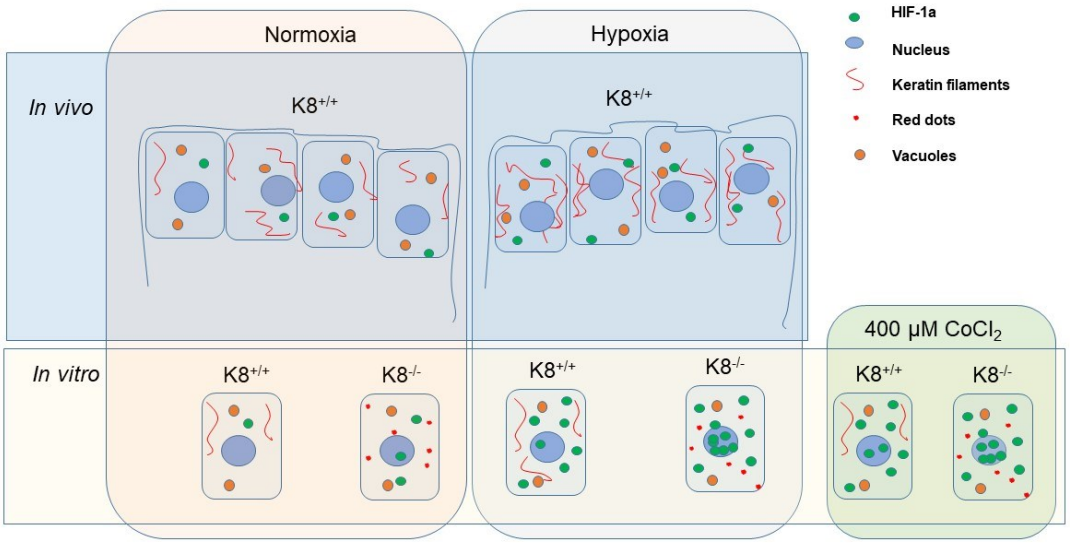

Figure 16. Keratins are up-regulated in hypoxia in colonic epithelial *in vivo* and *in vitro* in K8$^{+/+}$ mice and HIF-1a is translocated to nucleus in hypoxia *in vitro* in K8$^{-/-}$ cells. K19 and K20 are up-regulated in hypoxia in the colon epithelium more. K8 regulates localization of HIF-1a in normoxia and in hypoxia. HIF-1a is up-regulated and translocates to the nucleus in hypoxia in CRISPR-Cas9 K8$^{-/-}$ cells, compared to CRISPR/Cas9 K8$^{+/+}$ cells.

7. Future perspectives

This project was carried out to understand the role of intestinal keratins in the regulation of HIF-1a, HIF-2a and hypoxia signaling pathway in general. Various experiments were performed to understand the regulation of hypoxia signaling pathway and if keratins are the regulators of hypoxia signaling pathway. The general answer obtained the experiments conducted in this thesis project is that keratins are regulated in hypoxia and keratins regulate HIF-1a during hypoxia. There were many data produced during the project which were not studied enough and remained unanswered. For example, this study showed a link between keratins and HIF-1a in hypoxia but link between keratins HIF-2a is unclear. The role of keratins regarding regulation of HIF-2a is yet unknown and should be studied further.

An important next step is to understand the exact time-point of nuclear entry of HIF-1a as a function of K8. CRIPR/Cas9 Caco-2 $K8^{-/-}$ cells with both fixed cells staining (result not shown) and live cell imaging. Although the live cell imaging gave preliminary data for nuclear translocation of HIF-1a, the challenges for imaging and time limitation, the study remained incomplete and needs to be investigate further.

Interestingly, a preliminary study demonstrated that HIF-1a is up-regulated in cells when incubated with cell medium for 72 hours. There were not much study that linked medium consumption with HIF-1a and hypoxia signaling pathway. The preliminary data could open up the gateway to another factor regulating hypoxia signaling pathway. It would be very interesting to study if nutrient consumption can regulate both HIFs and keratins at the same time and should be investigated further.

8. Acknowledgements

I am very grateful to Diana Toivola for giving me the opportunity to work in her lab and perform my thesis work under her supervision. I am also thankful for her enormous support, guidance and attention towards my work. I want to thank Terhi Helenius, for all the help, supervision and suggestions for my thesis work and writing. It was a huge support and I really appreciate it. I am also thankful to my supervisor Iris Lähdeniemi for believing in me, for her valuable time, intense supervision and an all the help which she provided during my thesis work, writing and beyond.

I am thankful to all the members of Toivola laboratory for helping me with lab techniques and methods, especially Joel and Calle. Thanks to all other lab members as well. I would also like to thank Jari Korhonen and Jouko Sandholm for the help with microscopy and imaging. Thanks to BIMA coordinators, especially Joanna, for the help throughout my study.

I would also like to thank my husband, Anup Shrestha, for all the help during my Master's study and finalizing my thesis.

9. Supplementary figure

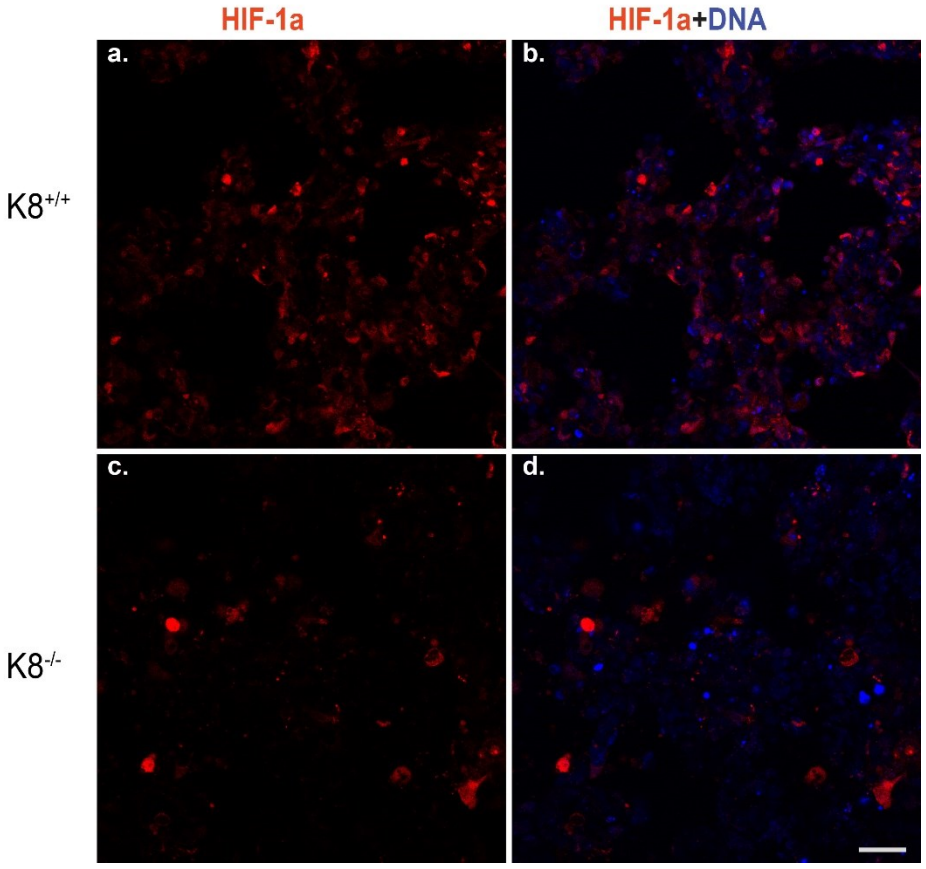

Figure 17. Increased transfection efficiency of CLIP-HIF-1a tag plasmid by transfecting the cells using Neon transfection system protocol. The CRISPR/Cas9 Caco-2 $K8^{+/+}$ and $K8^{-/-}$ cells were labeled with CLIP substrate at around 24 hours of transfection. The cells were imaged using confocal microscope without adding any chemical to induce hypoxia. The scale bar represents 50 µm length.

10. Appendix

Recipe and buffers

20 % SDS	
SDS	20 g
Dissolved in 1000 ml of dH_2O	

Homogenization buffer	
Tris-HCL	0.187 M (pH 6.8)
Ethylenediaminetetraacetate (EDTA)	5 mM

3X Laemmli buffer	
Glycerol	30%
SDS	30%
Bromphenol blue	0.015%
β-mercaptaethanol	3%
Tris-HCL	4.2 M

10X Running buffer	
Tris base	30 g
glycine	144 g
SDS	10 g
Dissolved in 1000 ml of dH_2O	
1 X running buffer was prepared by mixing 70 ml of 10X Running buffer and 5 ml of 20% SDS in 925 ml of dH_2O	
1 X transfer buffer was prepared by mixing 80 ml of 10X Running buffer, 5 ml of 20% SDS and 200 ml methanol in 715 ml of dH_2O	

10X Transfer buffer	
Tris base	30 g
glycine	144 g
SDS	10 g
Dissolved in 1000 ml of dH_2O	

0.2% PBS-Tween	
PBS tablets	20 g
Tween	4 ml
Dissolved in 2000 ml of dH_2O	

11. References

Alam, C.M., J.S.G. Silvander, E.N. Daniel, G.-Z. Tao, S.M. Kvarnström, P. Alam, M.B. Omary, A. Hänninen, and D.M. Toivola. 2013. Keratin 8 modulates β-cell stress responses and normoglycaemia. *J. Cell Sci.* 126:5635–5644.

Albenberg, L., T. Esipova, C. Judge, K. Bittinger, J. Chen, A. Laughlin, S. Grunberg, R. Baldassano, J. Lewis, H. Li, S. Thom, F. Bushman, S. Vinogradov, and G. Wu. 2014. Correlation Between Intraluminal Oxygen Gradient and Radial Partitioning of Intestinal Microbiota in Humans and Mice. *Gastroenterology*. 147:1055-1063.e8.

Alberts, B., A. Johnson, J. Lewis, M. Raff, K. Roberts, and P. Walter. 2007. *Molecular Biology of the cells. 5th ed*. Garland Science.

Asghar, M.N., S. Priyamvada, J.H. Nyström, A.N. Anbazhagan, P.K. Dudeja, and D.M. Toivola. 2016. Keratin 8 knockdown leads to loss of the chloride transporter DRA in the colon. *Am. J. Physiol. - Gastrointest. Liver Physiol.* 310:G1147–G1154.

Asghar, M.N., J.S.G. Silvander, T.O. Helenius, I.A.K. Lähdeniemi, C. Alam, L.E. Fortelius, R.O. Holmsten, and D.M. Toivola. 2015. The Amount of Keratins Matters for Stress Protection of the Colonic Epithelium. *PLoS ONE*. 10.

Balbi, V., and P. Ciarletta. 2013. Morpho-elasticity of intestinal villi. *J. R. Soc. Interface*. 10:20130109.

Baribault, H., J. Penner, R.V. Iozzo, and M. Wilson-Heiner. 1994. Colorectal hyperplasia and inflammation in keratin 8-deficient FVB/N mice. *Genes Dev.* 8:2964–2973.

Baribault, H., J. Price, K. Miyai, and R.G. Oshima. 1993. Mid-gestational lethality in mice lacking keratin 8. *Genes Dev.* 7:1191–1202.

Bhimji, S.S., and W.G. Gossman. 2017. Anatomy, Abdomen, Large Intestine. *In* StatPearls. StatPearls Publishing, Treasure Island (FL).

Borrelli, A., A.L. Tornesello, M.L. Tornesello, and F.M. Buonaguro. 2018. Cell Penetrating Peptides as Molecular Carriers for Anti-Cancer Agents. *Mol. Basel Switz.* 23.

Bragulla, H.H., and D.G. Homberger. 2009. Structure and functions of keratin proteins in simple, stratified, keratinized and cornified epithelia. *J. Anat.* 214:516–559.

Byndloss, M.X., and A.J. Bäumler. 2018. The germ-organ theory of non-communicable diseases. *Nat. Rev. Microbiol.* 16:103–110.

Chan, C.K., and P.M. Vanhoutte. 2013. Hypoxia, vascular smooth muscles and endothelium. *Acta Pharm. Sin. B*. 3:1–7.

Cole, N.B. 2013. Site-Specific Protein Labeling with SNAP-Tags. *Curr. Protoc. Protein Sci. Editor. Board John E Coligan Al*. 73:30.1.1-30.1.16.

Cole, R. 2014. Live-cell imaging. *Cell Adhes. Migr.* 8:452–459.

Cooper, G.M. 2000. *Intermediate Filaments*.

Crivat, G., and J.W. Taraska. 2012. Imaging proteins inside cells with fluorescent tags. *Trends Biotechnol.* 30:8–16.

Dahiru, T. 2008. P – VALUE, A TRUE TEST OF STATISTICAL SIGNIFICANCE? A CAUTIONARY NOTE. *Ann. Ib. Postgrad. Med.* 6:21–26.

Dengler, V.L., M. Galbraith, and J.M. Espinosa. 2014. Transcriptional Regulation by Hypoxia Inducible Factors. *Crit. Rev. Biochem. Mol. Biol.* 49:1–15.

Depping, R., A. Steinhoff, S.G. Schindler, B. Friedrich, R. Fagerlund, E. Metzen, E. Hartmann, and M. Köhler. 2008. Nuclear translocation of hypoxia-inducible factors (HIFs): Involvement of the classical importin α/β pathway. *Biochim. Biophys. Acta BBA - Mol. Cell Res.* 1783:394–404.

Di Franco, S., P. Mancuso, A. Benfante, M. Spina, F. Iovino, F. Dieli, G. Stassi, and M. Todaro. 2011. Colon Cancer Stem Cells: Bench-to-Bedside-New Therapeutical Approaches in Clinical Oncology for Disease Breakdown. *Cancers*. 3:1957–1974.

Donaldson, J.G. 2001. UNIT 4.3 Immunofluorescence Staining. *Curr. Protoc. Cell Biol. Editor. Board Juan Bonifacino Al*. 0 4:Unit-4.3.

Eales, K.L., K.E.R. Hollinshead, and D.A. Tennant. 2016. Hypoxia and metabolic adaptation of cancer cells. *Oncogenesis*. 5:e190.

Elson, D.A., G. Thurston, L.E. Huang, D.G. Ginzinger, D.M. McDonald, R.S. Johnson, and J.M. Arbeit. 2001. Induction of hypervascularity without leakage or inflammation in transgenic mice overexpressing hypoxia-inducible factor-1α. *Genes Dev.* 15:2520–2532.

Eltzschig, H.K., and P. Carmeliet. 2011. Hypoxia and Inflammation. *N. Engl. J. Med.* 364:656–665.

Garrett, W.S., J.I. Gordon, and L.H. Glimcher. 2010. Homeostasis and Inflammation in the Intestine. *Cell*. 140:859–870.

Gautier, A., A. Juillerat, C. Heinis, I.R. Corrêa, M. Kindermann, F. Beaufils, and K. Johnsson. 2008. An Engineered Protein Tag for Multiprotein Labeling in Living Cells. *Chem. Biol.* 15:128–136.

Griffiths, J.B. 1971. The Effect of Medium Changes on the Growth and Metabolism of the Human Diploid Cell, W1-38. *J. Cell Sci.* 8:43–52.

Guldiken, N., G. Kobazi Ensari, P. Lahiri, G. Couchy, C. Preisinger, C. Liedtke, H.W. Zimmermann, M. Ziol, P. Boor, J. Zucman-Rossi, C. Trautwein, and P. Strnad. 2016. Keratin 23 is a stress-inducible marker of mouse and human ductular reaction in liver disease. *J. Hepatol.* 65:552–559.

Helenius, T.O., C.A. Antman, M.N. Asghar, J.H. Nyström, and D.M. Toivola. 2016. Keratins Are Altered in Intestinal Disease-Related Stress Responses. *Cells*. 5.

Herrmann, H., and J.R. Harris. 1998. *Intermediate Filaments*. Springer Science & Business Media. 660 pp.

Höckel, M., and P. Vaupel. 2001. Tumor Hypoxia: Definitions and Current Clinical, Biologic, and Molecular Aspects. *JNCI J. Natl. Cancer Inst.* 93:266–276.

Huang, T., M. Long, and B. Huo. 2010. Competitive Binding to Cuprous Ions of Protein and BCA in the Bicinchoninic Acid Protein Assay. *Open Biomed. Eng. J.* 4:271–278.

Johansson, M.E.V., J.M.H. Larsson, and G.C. Hansson. 2011. The two mucus layers of colon are organized by the MUC2 mucin, whereas the outer layer is a legislator of host–microbial interactions. *Proc. Natl. Acad. Sci.* 108:4659–4665.

Karantza, V. 2011. Keratins in health and cancer: more than mere epithelial cell markers. *Oncogene*. 30:127–138.

Kellner, J.C., and P.A. Coulombe. 2009. Keratins and protein synthesis: the plot thickens. *J. Cell Biol.* 187:157–159.

Kim, T.K., and J.H. Eberwine. 2010. Mammalian cell transfection: the present and the future. *Anal. Bioanal. Chem.* 397:3173–3178.

Kretlow, J.D., Y.-Q. Jin, W. Liu, W.J. Zhang, T.-H. Hong, G. Zhou, L.S. Baggett, A.G. Mikos, and Y. Cao. 2008. Donor age and cell passage affects differentiation potential of murine bone marrow-derived stem cells. *BMC Cell Biol.* 9:60.

Ku, N.-O., J. Liao, and M.B. Omary. 1997. Apoptosis Generates Stable Fragments of Human Type I Keratins. *J. Biol. Chem.* 272:33197–33203.

Ku, N.-O., and M.B. Omary. 2006. A disease- and phosphorylation-related nonmechanical function for keratin 8. *J. Cell Biol.* 174:115–125.

Lee, J., K.-H. Jang, H. Kim, Y. Lim, S. Kim, H.-N. Yoon, I.K. Chung, J. Roth, and N.-O. Ku. 2013. Predisposition to apoptosis in keratin 8-null liver is related to inactivation of NF-κB and SAPKs but not decreased c-Flip. *Biol. Open*. BIO20134606.

Lee, Y.S., J. Kim, O. Osborne, D.Y. Oh, R. Sasik, S. Schenk, A. Chen, H. Chung, A. Murphy, S.M. Watkins, O. Quehenberger, R.S. Johnson, and J.M. Olefsky. 2014. Increased Adipocyte O2 Consumption Triggers HIF-1α Causing Inflammation and Insulin Resistance in Obesity. *Cell*. 157:1339–1352.

Li, S., T. Sun, and H. Ren. 2015. The functions of the cytoskeleton and associated proteins during mitosis and cytokinesis in plant cells. *Front. Plant Sci.* 6.

Liss, V., B. Barlag, M. Nietschke, and M. Hensel. 2015. Self-labelling enzymes as universal tags for fluorescence microscopy, super-resolution microscopy and electron microscopy. *Sci. Rep.* 5:17740.

Liu, C., E.-D. Liu, Y.-X. Meng, X.-M. Dong, Y.-L. Bi, H.-W. Wu, Y.-C. Jin, K. Zhao, J.-J. Li, M. Yu, Y.-Q. Zhan, H. Chen, C.-H. Ge, X.-M. Yang, and C.-Y. Li. 2017. Keratin 8 reduces colonic permeability and maintains gut microbiota homeostasis, protecting against colitis and colitis-associated tumorigenesis. *Oncotarget*. 8:96774–96790.

Luo, J.C., and M. Shibuya. 2001. A variant of nuclear localization signal of bipartite-type is required for the nuclear translocation of hypoxia inducible factors (1alpha, 2alpha and 3alpha). *Oncogene*. 20:1435–1444.

Ma, X., H. Zhang, X. Xue, and Y.M. Shah. 2017. Hypoxia-inducible factor 2α (HIF-2α) promotes colon cancer growth by potentiating Yes-associated protein 1 (YAP1) activity. *J. Biol. Chem.* 292:17046–17056.

Majmundar, A.J., W.J. Wong, and M.C. Simon. 2010. Hypoxia inducible factors and the response to hypoxic stress. *Mol. Cell*. 40:294–309.

de Mattos, B.R.R., M.P.G. Garcia, J.B. Nogueira, L.N. Paiatto, C.G. Albuquerque, C.L. Souza, L.G.R. Fernandes, W.M. da S.C. Tamashiro, and P.U. Simioni. 2015. Inflammatory Bowel Disease: An Overview of Immune Mechanisms and Biological Treatments. *Mediators Inflamm.* 2015.

Meran, L., A. Baulies, and V.S.W. Li. 2017. Intestinal Stem Cell Niche: The Extracellular Matrix and Cellular Components. *Stem Cells Int.* 2017.

Michiels, C. 2004. Physiological and Pathological Responses to Hypoxia. *Am. J. Pathol.* 164:1875–1882.

Misiorek, J.O. 2016. The role of keratin intermediate filaments in colon epithelial cells. Åbo Akademi University. 12–20 pp.

Misiorek, J.O., I.A.K. Lähdeniemi, J.H. Nyström, V.M. Paramonov, J.A. Gullmets, H. Saarento, A. Rivero-Müller, T. Husøy, P. Taimen, and D.M. Toivola. 2016. Keratin 8-deletion induced colitis predisposes to murine colorectal cancer enforced by the inflammasome and IL-22 pathway. *Carcinogenesis*. 37:777–786.

Motte, C.A.D. la, V.C. Hascall, J. Drazba, S.K. Bandyopadhyay, and S.A. Strong. 2003. Mononuclear leukocytes bind to specific hyaluronan structures on colon mucosal smooth muscle cells treated with polyinosinic acid: Polycytidylic acid. Inter-α-trypsin inhibitor is crucial to structure and function. *Am. J. Pathol.* 163:121–133.

Muz, B., P. de la Puente, F. Azab, and A.K. Azab. 2015. The role of hypoxia in cancer progression, angiogenesis, metastasis, and resistance to therapy. *Hypoxia*. 3:83–92.

Na, N., N.S. Chandel, J. Litvan, and K.M. Ridge. 2010. Mitochondrial reactive oxygen species are required for hypoxia-induced degradation of keratin intermediate filaments. *FASEB J. Off. Publ. Fed. Am. Soc. Exp. Biol.* 24:799–809.

Narula, N., and R.N. Fedorak. 2008. Exercise and inflammatory bowel disease. *Can. J. Gastroenterol.* 22:497–504.

Norwood, F.L., A.J. Sutherland-Smith, N.H. Keep, and J. Kendrick-Jones. 2000. The structure of the N-terminal actin-binding domain of human dystrophin and how mutations in this domain may cause Duchenne or Becker muscular dystrophy. *Structure*. 8:481–491.

Nowakowski, A.B., W.J. Wobig, and D.H. Petering. 2014. Native SDS-PAGE: High Resolution Electrophoretic Separation of Proteins With Retention of Native Properties Including Bound Metal Ions. *Met. Integr. Biometal Sci.* 6:1068–1078.

Okumura, R., and K. Takeda. 2017. Roles of intestinal epithelial cells in the maintenance of gut homeostasis. *Exp. Mol. Med.* 49:e338.

Omary, M.B. 2009. "IF-pathies": a broad spectrum of intermediate filament-associated diseases. *J. Clin. Invest.* 119:1756–1762.

Omary, M.B., N.O. Ku, J. Liao, and D. Price. 1998. Keratin modifications and solubility properties in epithelial cells and in vitro. *Subcell. Biochem.* 31:105–140.

Omary, M.B., N.-O. Ku, P. Strnad, and S. Hanada. 2009. Toward unraveling the complexity of simple epithelial keratins in human disease. *J. Clin. Invest.* 119:1794–1805.

Oshima, R.G. 2007. Intermediate Filaments: A Historical Perspective. *Exp. Cell Res.* 313:1981–1994.

Pfeiffer, S., J. Krüger, A. Maierhofer, Y. Böttcher, N. Klöting, N.E. Hajj, D. Schleinitz, M.R. Schön, A. Dietrich, M. Fasshauer, T. Lohmann, M. Dreßler, M. Stumvoll, T. Haaf, M. Blüher, and P. Kovacs. 2016. *Hypoxia-inducible factor 3A* gene expression and methylation in adipose tissue is related to adipose tissue dysfunction. *Sci. Rep.* 6:27969.

Planutis, K., M. Planutiene, and R.F. Holcombe. 2014. A novel signaling pathway regulates colon cancer angiogenesis through Norrin. *Sci. Rep.* 4:5630.

Prabhakar, N.R., and G.L. Semenza. 2015. Oxygen Sensing and Homeostasis. *Physiology*. 30:340–348.

Rao, J.N., and J.-Y. Wang. 2010. Intestinal Architecture and Development. Morgan & Claypool Life Sciences.

Regueiro, M.D., J.B. Greer, and S.B. Hanauer. 2016. Established Management Paradigms in IBD: Treatment Targets and Therapeutic Tools. *Am. J. Gastroenterol. Suppl.* 3:8–16.

Rossi, M., M. Jahanzaib Anwar, A. Usman, A. Keshavarzian, and F. Bishehsari. 2018. Colorectal Cancer and Alcohol Consumption-Populations to Molecules. *Cancers*. 10.

Sambuy, Y., I. De Angelis, G. Ranaldi, M.L. Scarino, A. Stammati, and F. Zucco. 2005. The Caco-2 cell line as a model of the intestinal barrier: influence of cell and culture-related factors on Caco-2 cell functional characteristics. *Cell Biol. Toxicol.* 21:1–26.

Santoyo-Ramos, P., M. Likhatcheva, E.A. García-Zepeda, M.C. Castañeda-Patlán, and M. Robles-Flores. 2014. Hypoxia-Inducible Factors Modulate the Stemness and Malignancy of Colon Cancer Cells by Playing Opposite Roles in Canonical Wnt Signaling. *PLoS ONE*. 9.

Shah, Y.M. 2016. The role of hypoxia in intestinal inflammation. *Mol. Cell. Pediatr.* 3.

Silvander, J.S.G., S.M. Kvarnström, A. Kumari-Ilieva, A. Shrestha, C.M. Alam, and D.M. Toivola. 2017. Keratins regulate β-cell mitochondrial morphology, motility, and homeostasis. *FASEB J. Off. Publ. Fed. Am. Soc. Exp. Biol.* 31:4578–4587.

Smyth, J.T., W.I. DeHaven, G.S. Bird, and J.W. Putney. 2007. Role of the microtubule cytoskeleton in the function of the store-operated Ca2+ channel activator, Stim1. *J. Cell Sci.* 120:3762–3771.

Snider, N.T., and M.B. Omary. 2014. Post-translational modifications of intermediate filament proteins: mechanisms and functions. *Nat. Rev. Mol. Cell Biol.* 15:163–177.

Steegenga, W.T., N.J. de Wit, M.V. Boekschoten, N. IJssennagger, C. Lute, S. Keshtkar, M.M.G. Bromhaar, E. Kampman, L.C. de Groot, and M. Muller. 2012. Structural, functional and molecular analysis of the effects of aging in the small intestine and colon of C57BL/6J mice. *BMC Med. Genomics*. 5:38.

Stoeltzing, O., M.F. McCarty, J.S. Wey, F. Fan, W. Liu, A. Belcheva, C.D. Bucana, G.L. Semenza, and L.M. Ellis. 2004. Role of Hypoxia-Inducible Factor 1α in Gastric Cancer Cell Growth, Angiogenesis, and Vessel Maturation. *JNCI J. Natl. Cancer Inst.* 96:946–956.

Tao, G.-Z., K.S. Looi, D.M. Toivola, P. Strnad, Q. Zhou, J. Liao, Y. Wei, A. Habtezion, and M.B. Omary. 2009. Keratins modulate the shape and function of hepatocyte mitochondria: a mechanism for protection from apoptosis. *J. Cell Sci.* 122:3851–3855.

Toivola, D.M., H. Baribault, T. Magin, S.A. Michie, and M.B. Omary. 2000. Simple epithelial keratins are dispensable for cytoprotection in two pancreatitis models. *Am. J. Physiol. Gastrointest. Liver Physiol.* 279:G1343-1354.

Toivola, D.M., P. Boor, C. Alam, and P. Strnad. 2015. Keratins in health and disease. *Curr. Opin. Cell Biol.* 32:73–81.

Toivola, D.M., S. Krishnan, H.J. Binder, S.K. Singh, and M.B. Omary. 2004. Keratins modulate colonocyte electrolyte transport via protein mistargeting. *J. Cell Biol.* 164:911–921.

Toivola, D.M., Q. Zhou, L.S. English, and M.B. Omary. 2002. Type II Keratins Are Phosphorylated on a Unique Motif during Stress and Mitosis in Tissues and Cultured Cells. *Mol. Biol. Cell*. 13:1857–1870.

Wells, J.M., O. Rossi, M. Meijerink, and P. van Baarlen. 2011. Epithelial crosstalk at the microbiota–mucosal interface. *Proc. Natl. Acad. Sci.* 108:4607–4614.

Wilson, K., and J.M. Walker. 2009. Principles and techniques of biochemistry and molecular biology. 7th ed. Cambridge University Press, Cambridge, UK : New York. 744 pp.

Wu, C., X. Zhu, W. Liu, T. Ruan, and K. Tao. 2017. Hedgehog signaling pathway in colorectal cancer: function, mechanism, and therapy. *OncoTargets Ther.* 10:3249–3259.

Xia, M., R. Huang, Y. Sun, G.L. Semenza, S.F. Aldred, K.L. Witt, J. Inglese, R.R. Tice, and C.P. Austin. 2009. Identification of Chemical Compounds that Induce HIF-1α Activity. *Toxicol. Sci.* 112:153–163.

Yuan, Y., G. Hilliard, T. Ferguson, and D.E. Millhorn. 2003. Cobalt Inhibits the Interaction between Hypoxia-inducible Factor-α and von Hippel-Lindau Protein by Direct Binding to Hypoxia-inducible Factor-α. *J. Biol. Chem.* 278:15911–15916.

Zeitouni, N.E., S. Chotikatum, M. von Köckritz-Blickwede, and H.Y. Naim. 2016. The impact of hypoxia on intestinal epithelial cell functions: consequences for invasion by bacterial pathogens. *Mol. Cell. Pediatr.* 3:14.

Zhdanov, A.V., I.A. Okkelman, F.W.J. Collins, S. Melgar, and D.B. Papkovsky. 2015. A novel effect of DMOG on cell metabolism: direct inhibition of mitochondrial function precedes HIF target gene expression. *Biochim. Biophys. Acta BBA - Bioenerg.* 1847:1254–1266.

Zheng, L., C.J. Kelly, and S.P. Colgan. 2015. Physiologic hypoxia and oxygen homeostasis in the healthy intestine. A Review in the Theme: Cellular Responses to Hypoxia. *Am. J. Physiol. - Cell Physiol.* 309:C350–C360.

Zhou, Q., D.M. Toivola, N. Feng, H.B. Greenberg, W.W. Franke, and M.B. Omary. 2003. Keratin 20 Helps Maintain Intermediate Filament Organization in Intestinal Epithelia. *Mol. Biol. Cell*. 14:2959–2971.

Zhu, C., J. Yu, Q. Pan, J. Yang, G. Hao, Y. Wang, L. Li, and H. Cao. 2016. Hypoxia-inducible factor-2 alpha promotes the proliferation of human placenta-derived mesenchymal stem cells through the MAPK/ERK signaling pathway. *Sci. Rep.* 6:35489.